

Dear Dr. Brovkin,

We appreciate your comments and have made minor revisions to address your concerns. We are also glad to know that our previous revisions have satisfactorily address the reviewers' concerns. We look forward to acceptance and publication of this manuscript upon your approval of these changes. Our specific responses are included below, followed by a highlighted manuscript indicating changes to the text.

Figure 1 now shows only the terrestrial feedbacks as implemented in this study, and the caption has been edited to reflect this change.

We encountered similar unintentional changes in land cover due to land conversion assumptions when we were trying to reproduce the historical period to generate a 2005 starting state. Not only did these changes have a large effect on the carbon cycle, but they dramatically changed the land cover trajectory. We resolved these problems by carefully mimicking the land conversion assumptions and reference land cover distributions as used by CESM in CMIP5. Luckily, we were dealing with just the land use change and not the dynamic vegetation, or else it might have been more difficult. It is important, however, to understand how both bioclimate and human land use interact to produce the spatial and temporal distribution of land cover. While we are not immediately tackling the challenge of integrating dynamic vegetation and land use in CESM/iESM, we do intend to explore effects on carbon and climate associated with land conversion assumptions such as preferential removal of forest when cropland or pasture are increased.

Figure 8 now includes a unit label for the color bar.

Line 420 has been corrected to read 'million km².'

As of yet there is no official word on the acceptance of LUMIP by the WGCM/WCRP. George expects to hear something soon, however.

Sincerely,
Alan (on behalf of the co-authors)

1 From land use to land cover: Restoring the afforestation signal in a coupled integrated
2 assessment - earth system model and the implications for CMIP5 RCP simulations
3
4 Alan V. Di Vittorio^{1,*}, Louise P. Chini², Ben Bond-Lamberty³, Jiafu Mao⁴, Xiaoying Shi⁴, John
5 Truesdale⁵, Anthony Craig⁵, Kate Calvin³, Andrew Jones¹, William D. Collins¹, Jae Edmonds³,
6 George C Hurtt², Peter Thornton⁴, Allison Thomson³

7
8 ¹Lawrence Berkeley National Laboratory, Berkeley, CA, USA
9 ²University of Maryland, College Park, MD, USA
10 ³Joint Global Change Research Institute, Pacific Northwest National Laboratory, College Park,
11 MD, USA

12 ⁴Climate Change Science Institute, Oak Ridge National Laboratory, Oak Ridge, TN, USA

13 ⁵Independent contractor with Lawrence Berkeley National Laboratory, Berkeley, CA, USA

14

15 ^{*}Lawrence Berkeley National Laboratory

16 Earth Sciences Division

17 One Cyclotron Road, Mail Stop 74R316C

18 Berkeley, CA 94720-8268

19 avdivittorio@lbl.gov

20

21 Abstract

22 Climate projections depend on scenarios of fossil fuel emissions and land use change, and the
23 IPCC AR5 parallel process assumes consistent climate scenarios across Integrated Assessment
24 and Earth System Models (IAMs and ESMs). The CMIP5 project used a novel “land use
25 harmonization” based on the Global Land use Model (GLM) to provide ESMs with consistent
26 1500-2100 land use trajectories generated by historical data and four IAMs. A direct coupling of
27 the Global Change Assessment Model (GCAM), GLM, and the Community ESM (CESM) has
28 allowed us to characterize and partially address a major gap in the CMIP5 land coupling design:
29 the lack of a corresponding land cover harmonization. For RCP4.5, CESM global afforestation is
30 only 22% of GCAM’s 2005 to 2100 afforestation. Likewise, only 17% of GCAM’s 2040
31 afforestation, and zero pasture loss, were transmitted to CESM within the directly coupled
32 model. This is a problem because GCAM relied on afforestation to achieve RCP4.5 climate
33 stabilization. GLM modifications and sharing forest area between GCAM and GLM within the
34 directly coupled model did not increase CESM afforestation. Modifying the land use translator in
35 addition to GLM, however, enabled CESM to include 66% of GCAM’s afforestation in 2040,
36 and 94% of GCAM’s pasture loss as grassland and shrubland losses. This additional afforestation
37 increases CESM vegetation carbon gain by 19 PgC and decreases atmospheric CO₂ gain by 8
38 ppmv from 2005 to 2040, which demonstrates that CESM without additional afforestation
39 simulates a different RCP4.5 scenario than prescribed by GCAM. Similar land cover
40 inconsistencies exist in other CMIP5 model results, primarily because land cover information is
41 not shared between models. Further work to harmonize land cover among models will be
42 required to increase fidelity between IAM scenarios and ESM simulations and realize the full
43 potential of scenario-based earth system simulations.

44 1. Introduction

45 Land use plays a major role in determining terrestrial-atmosphere mass and energy
46 exchange (Adegoke et al., 2007; Raddatz, 2007), which in turn influences local to global climate
47 (Brovkin et al., 2013; Jones et al., 2013a; Pitman et al., 2009). Despite much recent progress, we
48 still have a limited understanding of how historical land use has affected, and continues to affect,
49 climate (Brovkin et al., 2013; Jones et al., 2013a; Pitman et al., 2009) and carbon (Anav et al.,
50 2013; Arora and Boer, 2010; Houghton, 2010; Houghton et al., 2012; Hurtt et al., 2006; Jain et
51 al., 2013; Jain and Yang, 2005; Jones et al., 2013b; Smith and Rothwell, 2013), and high
52 uncertainty as to how land use might evolve in the future (Hurtt et al., 2011; van Vuuren et al.,
53 2011a; Wise et al., 2009). Part of the uncertainty in future land use trajectories is due to inherent
54 unpredictability of human actions, and part to the high diversity of potential climate mitigation
55 and adaptation scenarios. Several energy and land strategies have been proposed to mitigate
56 climate change (Rose et al., 2012; Smith et al., 2013a), and while these strategies have similar
57 overall goals, some strategies will likely compete for land and other resources if implemented
58 simultaneously. For example, afforestation and bioenergy production both aim to reduce
59 atmospheric CO₂ concentrations, but both activities require land area, and both strategies would
60 impact crop production and markets through effects on crop area (Reilly et al., 2012).

61 Reflecting this limited understanding of land use effects on climate and carbon, Global
62 Climate Models (GCMs), and also next generation Earth System Models (ESMs) that include
63 fully coupled atmosphere-land-ocean carbon cycles, implement a wide range of land use/cover
64 approaches with varying degrees of detail and limited inclusion of managed ecosystems and land
65 use practices (Brovkin et al., 2013; Pitman et al., 2009). The Land Use and Climate,
66 IDentification of robust impacts (LUCID) activity employed seven GCMs to determine whether

67 land use change has significant regional climate impacts and farther-reaching teleconnections
68 due to biophysical changes in land surface. The results for 1972-2002 revealed significant but
69 inconsistent changes in temperature, precipitation, and latent heat in some areas where land use
70 change had occurred. The authors concluded that the model disagreement was due mainly to
71 differences in land use and land cover change implementations and corresponding land cover
72 distributions, with contributions from methodological differences in crop phenology, albedo, and
73 evapotranspiration (Pitman et al., 2009). The environmental factors addressed by LUCID are
74 also key factors for determining carbon uptake by vegetation, and thus it is not surprising that the
75 Coupled Climate-Carbon Cycle Model Intercomparison Project (C⁴MIP) activity generated ESM
76 projections that range from the land being a carbon source to a large carbon sink by 2100
77 (Friedlingstein et al., 2006).

78 To advance the scientific understanding of the effects of land use change on climate,
79 phase 5 of the Coupled Model Intercomparison Project (CMIP5) (Taylor et al., 2012) applied a
80 novel “land use harmonization” approach to produce the required land use change information
81 for all participating GCMs and ESMs. The Global Land use Model (GLM) was used for this land
82 use harmonization to generate the first set of continuous, spatially gridded land use change
83 scenarios for the years 1500-2100 (Hurtt et al., 2011). GLM computes land use states and
84 transitions annually at half-degree, fractional spatial resolution, including secondary land age,
85 area, and biomass, and the spatial patterns of shifting cultivation and wood harvesting (Hurtt et
86 al., 2006). Land use products from GLM have successfully been used as inputs to both regional
87 and global dynamic land models (Baidya Roy et al., 2003; Hurtt et al., 2002; Shevliakova et al.,
88 2009) and fully coupled ESMs (Jones et al., 2011; Shevliakova et al., 2013). The land use

89 harmonization process ensures a continuous transition from the historical reconstructions to the
90 future projections made by Integrated Assessment Models (IAMs).

91 The land use harmonization methodology was designed to satisfy the demands of a broad
92 range of models and to provide a consistent set of land use inputs for GCMs and ESMs. The
93 historical period of the land use harmonization (1500-2005) was based on version 3.1 of the
94 Historical Database of the Environment (HYDE; Klein Goldewijk et al., 2011) and Food and
95 Agriculture Organization (FAO) wood harvest data. For the future period (2005-2100), the land
96 use harmonization process utilized land use data from the four Representative Concentration
97 Pathways (RCPs), each provided by a different IAM. The RCP scenarios were designed to each
98 meet a different radiative forcing target (2.6, 4.5, 6.0, and 8.5 W m⁻²), and due to differences
99 among the IAMs these scenarios spanned a range of approaches in all sectors, including land use,
100 for meeting the targets (van Vuuren et al., 2011a). As a result, forest cover change varied widely
101 from deforestation to afforestation across the scenarios. Once the land use data were passed
102 through the land use harmonization, each GCM/ESM utilized a unique subset of the harmonized
103 outputs, based on model capabilities, and applied it to a unique set of land use and land cover
104 types (e.g. Lawrence et al., 2012). Although this process was largely successful in enabling the
105 first spatially explicit land use driven climate change experiments, it introduced considerable
106 uncertainty into the climate response for a given RCP in part because of model-specific
107 translation requirements between harmonized land use outputs and GCM/ESM simulated land
108 cover. This uncertainty due to inconsistent land cover distributions among models precluded
109 robust intercomparison of land-atmosphere processes (e.g., carbon uptake, evapotranspiration)
110 because differences among models were dominated by the differences among simulated land
111 cover distributions (Brovkin et al., 2013). As land use and land cover are interdependent, a more

112 detailed specification of the relationship between land use and land cover may reduce uncertainty
113 in earth system simulations such that experiments can focus on land-atmosphere process
114 uncertainty rather than be confounded by inconsistent land use/cover distributions.

115 Recent analyses of CMIP5 results using prescribed CO₂ concentrations have also showed
116 the land ranging from a carbon source to a sink in 2100 for a given scenario (Brovkin et al.,
117 2013; Jones et al., 2013b). The LUCID activity was repeated for five CMIP5 ESMs and the
118 results demonstrated that large inter-model spreads of key regional land surface variables
119 (temperature, precipitation, albedo, latent heat, and available energy) were still due mainly to
120 differences in land use and land cover change implementations and corresponding land cover
121 distributions. Inter-model spreads of CO₂ emissions, however, were attributed mainly to
122 differences in land carbon cycle process parameterizations. As a result, different land cover
123 distributions among the models gave significantly different regional changes in climate
124 associated with land use change, but with insignificant effects on global mean temperature.
125 Furthermore, the range of net cumulative land use change emissions from 2006 to 2100 for
126 RCP8.5 was 34 to 205 PgC, with the high estimate likely due to the combination of relatively
127 high levels of land carbon and the inclusion of all land use transitions rather than just net land
128 use change (Brovkin et al., 2013). Additionally, not all of the models used the GLM wood
129 harvest data, further contributing to the spread of model results. For comparison, estimates of net
130 cumulative carbon emissions during 1700-2000 (1850-2000) range from 138-250 PgC (110-210
131 PgC) (Table 3 in Smith and Rothwell, 2013). The differences in land use and land cover
132 implementations are also a main factor in the large spread of 21st century land carbon uptake and
133 of compatible fossil fuel emissions allowable for a given RCP. In fact, the inter-model spreads in
134 land carbon uptake for individual scenarios are greater than the inter-scenario spreads for

135 individual models (Jones et al., 2013b). It is apparent that further work is needed to resolve
136 inconsistencies among land use and land cover approaches to reduce climate uncertainty,
137 especially for regional impact assessment.

138 Additional sources of climate uncertainty related to land use are the RCP radiative
139 forcing targets, which include only emissions of GreenHouse Gases (GHGs) and some aerosols
140 and reactive gases (van Vuuren et al., 2011a). These targets do not include radiative forcing from
141 albedo change or other direct climate effects associated with land use change. In a recent
142 modeling experiment, two different carbon tax policies with dramatically different land use
143 scenarios met the same radiative forcing target (4.5 W m^{-2}) in the IAM used for RCP4.5 but had
144 significantly different radiative forcing in an ESM (difference of 1 W m^{-2}) due to albedo
145 differences between the land use scenarios (Jones et al., 2013a). Likewise, the Shared
146 Socioeconomic Pathways (SSPs) for mitigation, adaptation, and impact studies in the
147 Intergovernmental Panel on Climate Change (IPCC) fifth Assessment Report (AR5) are likely to
148 produce different land use scenarios that meet the same RCP target, but have different radiative
149 forcing in the ESMs due to the direct effects of land use and land cover change on climate.
150 However, one of the goals of the RCP process was to provide a set of radiative forcing targets for
151 ESMs that remains consistent with respect to the diversity of SSPs associated with each RCP
152 target (Moss, et al., 2010). As a result of the wide range of land use and land cover related
153 uncertainties in climate projections, an increased emphasis on land use and land cover dynamics
154 is a high priority for CMIP6 (Meehl et al., 2014).

155 A more consistent and complete land use and land cover coupling between IAMs and
156 ESMs will facilitate more accurate projections of global change scenarios and more robust multi-
157 model intercomparisons of climate and carbon cycle interactions with anthropogenic drivers such

158 as fossil fuel emissions and land use change. These expected outcomes are in line with a primary
159 goal of a scenario-based approach, such as the RCPs, which is “to better understand uncertainties
160 in order to reach decisions that are robust under a wide range of possible futures” (Moss et al.,
161 2010; p. 747). The RCPs were designed to better understand uncertainties in global climate
162 projections by providing distinct scenarios of atmospheric radiative forcing and land use change.
163 Intra-scenario comparison of ESM simulations offers insights to uncertainties in ESM processes,
164 while inter-scenario comparison of ESM simulations offers insights to uncertainties due to a
165 range of possible futures. However, the efficacy of this approach depends on the fidelity of the
166 ESM simulations to the RCP scenarios. Without this fidelity, intra-scenario comparison is not
167 possible, because the ESMs are not simulating the same scenario, and inter-scenario comparison
168 might include futures outside the prescribed range of possibility.

169 The IAMs projected a complete terrestrial surface (along with ice, rock, and urban) for
170 each given scenario because land use and land cover are interdependent. For example, carbon
171 stocks in various ecosystems might be valued under a carbon price policy, so land cover would
172 need to be determined along with land use. Or a land policy might restrict certain land cover
173 conversions. Within the CMIP5 coupling process, however, GCMs and ESMs determine their
174 own land cover while remaining consistent with the land use harmonization data, thus
175 potentially reducing the fidelity of the full climate simulations to the RCP scenarios. This
176 was a practical design that obviated the redesign of GCM/ESM land use and land cover
177 implementations, but also precluded analysis of the climate impacts of different land cover
178 responses to land use change because such analysis is robust only within a single model where
179 everything but land cover response remains consistent. Another challenge posed by the
180 interdependence of land use and land cover is the implementation of geographic shifts in land

181 cover due to bioclimatic changes. While these shifts are often implemented within ESMs, such
182 shifts are a second-order effect that is superposed upon land use change and might be better
183 implemented as a feedback from ESMs to IAMs to inform land use and land cover projection.
184 Incorporating both land use and land cover into the coupling between IAMs and ESMs is a
185 fundamental step toward realizing the full potential of the scenario-based RCP process.

186 Our approach to addressing inconsistencies between IAMs and ESMs is to integrate an
187 IAM and an ESM into the first fully coupled model that directly simulates human-environment
188 feedbacks. The resulting integrated ESM (iESM) includes climate feedbacks on vegetation
189 productivity and ecosystem carbon from the Community ESM (CESM) to the Global Change
190 Assessment Model (GCAM) to facilitate land use projection at five-year intervals. The iESM
191 uses GLM as in the CMIP5 land use harmonization, along with the CESM Land Use Translator
192 (LUT) that converts land use harmonization outputs to CESM land cover and wood harvest area.
193 Our initial iESM simulations showed that time varying factors based on CESM simulated Net
194 Primary Production (NPP) and Heterotrophic Respiration (HR) were successfully used by
195 GCAM for land use projection. However, these simulations also demonstrated that the large
196 RCP4.5 afforestation signal was not being passed through from GCAM to CESM. GCAM
197 simulated afforestation as a carbon-sequestering strategy to help meet the RCP4.5 target, but this
198 additional forest area was not included in the land use harmonization. As a result, most of this
199 forest area was not included in CESM simulations, both for CMIP5 and in an early version of
200 iESM.

201 Here we test the feasibility of restoring the lost afforestation signal by using the iESM as
202 a test bed to explore alternative coupling strategies. We focus on modifications to the CESM
203 LUT because initial modifications to GLM did not restore CESM afforestation. One advantage

204 of focusing on a post-land use harmonization approach is that it could be applied to other ESMs
205 independently without changing the land use harmonization product. Section 2 includes model
206 description and experimental design, Section 3 presents results and demonstrates that this
207 problem exists in CMIP5, and Section 4 discusses the limitations of our current approach and the
208 implications for the CMIP5 archive with respect to land use and climate. We conclude with
209 suggestions for improving IAM to ESM land coupling for future model inter-comparisons.

210

211 2. Methods

212 2.1. iESM Description

213 The iESM integrates GCAM, GLM, and CESM to evaluate the effects of human-
214 environment feedbacks on the earth system (Figure 1). We have completed the first coupling
215 stage that allows GCAM to project land use distribution in five-year increments based on the
216 previous five years of CESM vegetation productivity. Here we give an overview of how the three
217 main components interact. A more detailed description of iESM development will be presented
218 in a forthcoming paper (Collins et al., in prep.).

219 GCAM v3.0 ((Calvin et al., 2011); henceforth referred to as GCAM) is a tightly coupled
220 IAM of human and biogeophysical processes associated with climate change. GCAM's human
221 system components simulate global economic activity within energy, agriculture, and forest
222 product markets with respect to 14 geopolitical regions. A previous version of GCAM projected
223 land use and land cover distributions for each of the 14 geopolitical regions (Wise et al., 2009)
224 and was used to generate the CMIP5 RCP4.5 scenario (Thomson et al., 2011). Currently, GCAM
225 incorporates a range of improvements to the Agriculture and Land Use (AgLU) module,
226 including the capacity to operate on 151 geographical land units to generate a more detailed and

227 accurate spatial distribution of land use. There are three land cover types that remain constant
228 over time (urban, tundra, and rock/ice/desert) and 24 land use and land cover types available for
229 redistribution, including 12 food and feed crops, five bioenergy crops, and seven managed and
230 unmanaged ecosystems (Kyle et al., 2011; Wise and Calvin, 2011). The “geographical land
231 units” are defined by intersecting 18 global agro-ecological zones (Lee et al., 2005) with the 14
232 geopolitical regions. In the iESM, GCAM projects land use and land cover distributions within
233 each of these land units at five-year intervals. These distributions are based on profit shares
234 calculated from agricultural costs, prices, yields, and the application of a carbon price to
235 vegetation and soil carbon densities.

236 In a second and intermediate step, GLM uses GCAM’s cropland, pasture, and forest areas
237 (and wood carbon harvest) to compute all annual, fractional land use states and transitions. As
238 part of this process it disaggregates GCAM’s geographical land unit data to a half-degree global
239 grid by computing spatial patterns and also ensures consistency with the historical land use
240 reconstructions (Hurtt et al., 2011; Hurtt et al., 2006). GLM has been slightly modified from its
241 CMIP5 implementation to better facilitate forest area change matching with GCAM (Section
242 2.3.2). This modification enables GLM to use forest area output from GCAM that was not
243 incorporated into the CMIP5 land use harmonization. Nonetheless, iESM still follows the CMIP5
244 implementation for CESM in using these GLM land use harmonization outputs: cropland,
245 pasture, primary, and secondary land area, as well as wood harvest areas on primary and
246 secondary forested and non-forested land.

247 CESM (Bitz et al., 2011; Gent et al., 2011) has fully coupled atmosphere, ocean, land,
248 and sea ice components. Within CESM, the Community Land Model v4.0 (CLM; Lawrence et
249 al., 2011) receives the selected GLM outputs via a translator that converts these outputs to 16

250 CLM Plant Functional Types (PFTs; eight forest, three grass, three shrub, one bare soil, and one
251 crop) (Lawrence et al., 2012). The CLM dynamic vegetation module, which estimates
252 bioclimate-driven geographical shifts in CLM PFTs, cannot run at the same time as the land use
253 change module presented here; only one of these modules can change CLM PFT areas per
254 simulation. While the iESM does not directly estimate bioclimatic shifts in land cover, the NPP
255 and HR feedbacks to GCAM do incorporate bioclimatic effects on ecosystems into GCAM's
256 land use cover projections. The version of iESM used in this study was based on CESM
257 v1.0beta9, which is a pre-release version of the model used for the CMIP5 simulations.

258 The iESM climate feedbacks on vegetation and carbon were implemented by passing
259 annual climate scaling factors from CESM to GCAM based on NPP and HR. These factors were
260 used to scale GCAM crop yields and vegetation and soil carbon densities every five years. To
261 calculate the scaling factors, the per-pixel, PFT-specific CESM 5-year annual average NPP and
262 HR values for a given GCAM time step were divided by base-period average annual values
263 (1990-2004). These NPP and HR ratios were then filtered to exclude outliers based on a median
264 absolute deviation method, and finally aggregated to GCAM's geographical land units and land
265 use and land cover types (for details see Bond-Lamberty et al., in review). Crop yields and
266 vegetation carbon densities for GCAM's next land use projection were scaled by the NPP ratio,
267 while soil carbon densities were scaled by a combination of the NPP and HR ratios ($(NPP_{ratio} +$
268 $(1 - (HR_{ratio} - 1))) / 2$).

269

270

271

272

273 2.2. Simulations

274 Our iESM simulations cover 2005 to 2040 with fully coupled CESM components and
275 prescribed RCP4.5 emissions and carbon price path. These simulations use the land use change
276 module, a dynamic ocean (Smith et al., 2013b), Community Atmosphere Model v4 physics
277 (Gent et al., 2011), carbon-nitrogen biogeochemistry (Thornton et al., 2007), and active land-
278 atmosphere-ocean carbon dynamics, at approximately 1° resolution (0.9375°x1.25°). The iESM
279 initial conditions are the culmination of a CESM spinup run followed by a CESM 1850-2005
280 transient historical run with land use change. GCAM initial conditions are calibrated to 2005
281 wood harvest, land use area, and energy and agriculture costs and production, as reported by
282 individual countries and processed and archived by international organizations (e.g. FAO,
283 International Energy Agency). The GCAM RCP4.5 scenario was described fully by Thomson et
284 al. (2011).

285 We performed two fully integrated simulations to compare two iESM cases: 1) original
286 CESM land use translator (OLDLUT) and 2) modified CESM land use translator (NEWLUT)
287 (Table 1). In fact, OLDLUT was our initial fully integrated simulation with iESM and, as
288 reported below, it revealed inconsistencies within iESM that needed to be addressed prior to
289 scientific experimentation. OLDLUT also showed that the updated GLM did not increase CESM
290 afforestation with respect to a previous simulation performed by manually passing data between
291 the respective iESM models. The NEWLUT case was used to test our hypothesis that the lost
292 afforestation signal could be recovered by modifying only the CESM component of iESM. These
293 fully integrated runs included climate feedbacks on vegetation productivity and ecosystem
294 carbon in GCAM's land use projections, which occurred at five-year intervals. Analysis of the

295 effects of introducing these feedbacks on land use, carbon, and climate will be presented in a
296 forthcoming paper (Thornton et al, in prep).

297

298 2.3. Land use coupling

299 2.3.1. OL_DLUT land use coupling within iESM

300 The OL_DLUT iESM land use coupling followed the CMIP5 land use harmonization
301 algorithm (Figure 2), but with a slightly modified version of GLM (see Section 2.3.2). The
302 coupling was designed to match GCAM and CESM changes in absolute cropland and pasture
303 area. For CMIP5, GLM received only crop and pasture areas from GCAM, but for the iESM
304 GLM also receives forest area from GCAM to better facilitate forest area change matching (see
305 Section 2.3.2). GLM also receives wood products demand from GCAM (in tons of carbon),
306 which is spatially distributed to determine the extent of harvested area in each of five wood
307 harvest types (primary forest harvest, primary non-forest harvest, secondary mature forest
308 harvest, secondary immature forest harvest, and secondary non-forest harvest). The OL_DLUT
309 (Figure 3) uses only the cropland and pasture area outputs from GLM to update CESM PFT
310 areas in conjunction with maps of potential vegetation (the vegetation most likely to be present if
311 no land use change had occurred; Ramankutty and Foley, 1999). Non-crop PFT area reductions
312 are made in proportion to their respective existing grid-cell fractions, while additions are made in
313 proportion to their respective potential vegetation grid cell fractions. The OL_DLUT does not use
314 the primary and secondary land area information for updating PFT areas because CESM does not
315 keep track of these land use designations. The OL_DLUT does, however, use the primary and
316 secondary land area to calculate the harvested fraction of GLM harvestable area (sum of the five
317 wood harvest type areas divided by the total area of primary and secondary land). Wood is

318 harvested from only forest in CESM, and so the GLM harvested fraction is applied to forest area
319 to determine the harvested area in CESM (Lawrence et al., 2012).

320 The OLDSLUT makes specific assumptions about pasture area change because CESM
321 does not keep track of pasture area (Figure 3). Changes in GLM cropland result directly in
322 CESM changes in crop PFT area, but changes in pasture area are constrained by forest PFT area
323 and reflected in changes in grass and shrub PFT area. More specifically, pasture addition is
324 limited to replacement of existing forest PFT area with grass PFT area, and pasture removal is
325 limited to the replacement of grass and shrub PFT area by potential forest PFT area. This means
326 that grass and shrub PFT area changes associated with pasture area change can be only as large
327 as the available existing or potential forest area.

328

329 2.3.2. Modifying the GLM spatial distribution algorithm

330 For the iESM, GLM was modified to better facilitate forest area change matching with
331 GCAM in an effort to increase the forest area simulated by CESM. These modifications included
332 operating on GCAM's 151 geographical land units (rather than the 14 regions used for CMIP5)
333 in addition to using GCAM's forest area output, which was not previously shared between the
334 models. For CMIP5, GLM applied the cropland and pasture area changes to the 2005 half-degree
335 map of cropland and pasture while preserving the total cropland and pasture area changes within
336 GCAM regions. Spatial allocation of cropland and pasture areas to the half-degree grids was
337 done with a preference for expanding agricultural area onto non-forested land and reducing
338 agricultural area where GLM would expect a forest to grow, while also preserving 2005 spatial
339 patterns of land use by allocating new cropland and pasture near to existing agricultural areas
340 (Hurt et al., 2011).

341 The new GLM algorithm uses GCAM forest area from each geographical land unit at
342 each time step and attempts to preserve the forest area changes within each geographical land
343 unit in addition to preserving the cropland and pasture area changes. GLM has previously
344 defined "forest" as natural vegetation that is growing on land where the potential biomass
345 density, based on an internal potential vegetation growth model, is greater than 2 kgC m^{-2} . Using
346 this definition the potential forestland within GLM is fixed and, as a result, the GLM algorithm
347 cannot grow forest outside of this forestland. In the new algorithm, GLM matches GCAM forest
348 area changes by moving cropland and pasture around within each geographical land unit to
349 "expose" enough potential forestland for regrowth to meet the GCAM forest area changes (see
350 the following steps a-c). In addition, to meet GCAM's land requirements for afforestation,
351 GLM uses a different definition of "forest" (potential biomass density greater than 1 kgC m^{-2} ,
352 rather than 2 kgC m^{-2}) than the definition used elsewhere in the GLM code (e.g. for computing
353 the spatial pattern of wood harvesting). The new GLM algorithm operates in three main steps:
354 a) Decreases in cropland and pasture occur first on the highest potential biomass land and
355 increases in cropland and pasture occur first on the lowest potential biomass land.
356 b) If the forest area change within a geographical land unit is not met, a redistribution of
357 cropland and pasture within that geographical land unit occurs such that, when possible,
358 existing cropland and pasture is moved from high biomass density land to low biomass
359 density land.
360 c) If the forest area change within a geographical land unit is still not met, the algorithm
361 attempts to allocate any "unmet" forest area change within another land unit (or across
362 multiple land units) within the same region, using a similar method to (b) above.
363

364 2.3.3. Modifying the CESM land use translation algorithm

365 To test our hypothesis that the lost afforestation signal could be recovered solely by the

366 ESM component, we focused on modifying the LUT (NEWLUT; Figure 4) to capture GCAM

367 afforestation via changes in agricultural land. This approach is more expedient than redesigning

368 the coupling code and LUT to receive forest area changes directly from GLM because such

369 redesign would logically require implementation of a single, consistent land surface and carbon

370 cycle among all iESM components. Specifically, the NEWLUT adds tree PFTs when cropland

371 and pasture are removed. Furthermore, the NEWLUT preferentially removes tree PFTs when

372 cropland and pasture are added. Forest area information is still not shared between GLM and the

373 NEWLUT (other than forest harvest). The NEWLUT also includes proper grid cell fraction

374 matching between GLM and CESM, which primarily affects crop, grass, and shrub PFTs.

375

376 2.3.3. CMIP5 RCP4.5 land use and land cover distributions among GCAM, GLM, and CESM

377 The OLDLUT iESM land use coupling was also used in CMIP5, albeit with 14 regions

378 rather than 151 geographical land units and without the GLM modifications and climate

379 feedbacks described above, and so we explored the extent to which the afforestation signal was

380 lost in the CMIP5 simulations. We compared the RCP4.5 pre-land use harmonization forest and

381 pasture area outputs from GCAM with the GLM land use harmonization values and also with the

382 corresponding PFT area inputs for the CESM1.0-BGC simulations submitted to the CMIP5

383 archive. CESM1.0-BGC served as the base code for iESM and thus contains the same versions

384 of the model components.

385

386

387 3. Results

388 3.1. CMIP5 RCP4.5 land use and land cover area inconsistencies

389 The GCAM afforestation signal was dramatically decreased in the CESM simulations,

390 and the total area covered by CESM herbaceous (grass and shrub) PFTs increased while

391 GCAM pasture decreased (Figure 5). CESM forest area increased by 23% of the 4.82 million

392 km² of afforestation between 2005 and 2020, and by 22% of the 10.98 million km² of

393 afforestation, by 2100. GLM captured 64% and 56% of the afforestation in 2020 and 2100,

394 respectively. GCAM and GLM pasture decreased by 4.69 million km² from 2005 to 2100

395 while CESM herbaceous PFTs increased by 1.11 million km² over the same period. The

396 changes in global cropland area were faithfully transmitted (CESM decreases were only 7%

397 less than GCAM decreases), but absolute CESM cropland area was approximately 1.5

398 million km² less than GCAM cropland area throughout the simulation (data not shown).

399 Changes in GLM pasture and cropland areas were essentially identical to GCAM changes,

400 and GLM absolute area values were slightly higher and lower, respectively, than GCAM

401 pasture and cropland areas (cropland data not shown).

402

403 3.2. Restored afforestation in iESM

404 The OLDSLUT simulation revealed that only changes in crop area were being faithfully

405 transmitted from GCAM to CESM (Figure 6; changes in global area). In contrast, CESM forest

406 area increased by only 17% of GCAM's 5.40 million km² of afforestation between 2015 and

407 2020, and by only 17% of the 7.73 million km² of afforestation between 2015 and 2040. Changes

408 in GLM forest area, on the other hand, reflected changes in GCAM forest area quite well (Figure

409 6), but at the cost of dramatically overestimating absolute forest area within GLM due to a low

410 biomass threshold for defining forest (Figure 7; absolute values of global area). Within GLM, the
411 new algorithm captured 93% of afforestation between 2015 and 2020 and 84% between 2015
412 and 2040, as compared to the original GLM algorithm that captured only 14% and 20% over the
413 respective periods in a previous simulation performed by manually passing data between the
414 respective iESM models (data not shown). Changes in GCAM pasture were not reflected by
415 changes in CESM herbaceous PFTs, but were faithfully output by GLM (Figure 6).

416 The NEWLUT simulation shows improved forest and cropland area changes in CESM
417 with a corresponding change in CESM herbaceous PFT area. The main improvement is that
418 CESM forest area increases by 64% of GCAM's 2015-2020 afforestation and by 66% of the 7.71
419 million km² of afforestation from 2015-2040 (Figure 6). This additional forest area in NEWLUT
420 reduces total area covered by CESM herbaceous PFTs by 94% of the 4.36 million km² of GCAM
421 pasture loss by 2040. Figure 8 shows the spatial tradeoff between forest and herbaceous PFTs
422 that achieves this level of afforestation, and Figure 9 demonstrates a sustained increase in
423 average annual land carbon uptake after 2020 due to additional afforestation. In comparison to
424 OL_DLUT, the NEWLUT increase in land carbon uptake results in a 19 PgC increase in
425 vegetation carbon gain and an 8 ppmv decrease in atmospheric CO₂ gain between 2005 to 2040
426 (Figure 10). NEWLUT also improves the CESM absolute cropland area (Figure 7) through
427 proper matching of GLM and CESM grid cell fractions. The effect of this proper matching is
428 apparent in the cropland and pasture area changes from 2005 to 2006 (Figures 6 and 7). GLM
429 NEWLUT outputs follow the GCAM NEWLUT outputs with relationships between GLM and
430 GCAM similar to those for OL_DLUT (data not shown).

431

432

433 4. Discussion

434 The iESM and CMIP5 land cover area discrepancies (Figures 5-7) result from a gap in
435 the original CMIP5 land coupling design that allows inconsistent forest area and land cover type
436 definitions across models (Figure 2), along with different underlying carbon cycles. The land use
437 harmonization was, however, ambitious and largely successful in developing consistent land use
438 definitions and data without requiring extensive redevelopment of land use and land cover
439 components of all participant models (Hurt et al., 2011). As our study attests, such
440 redevelopment is challenging and model-specific, but might be required for ESMs to adequately
441 simulate the IAM-prescribed anthropogenic drivers and their corresponding effects on carbon
442 and climate. Thus, while this is a specific case, the lost iESM afforestation signal is instructive of
443 the shortcomings of the CMIP5 design and the restoration of this signal offers insights into
444 improving land use and land cover coupling for model inter-comparisons.

445 A primary challenge for improving the CMIP5 land coupling is to increase the amount of
446 specific land cover information being shared between IAM (and historical) scenarios and ESMs.
447 For CMIP5, the land use harmonization was designed to harmonize land use data between
448 models, and as such GLM did not receive forest area or any other land cover information from
449 any of the IAMs (Masui et al., 2011; Riahi et al., 2011; Thomson et al., 2011; van Vuuren et al.,
450 2011b). Thus, at the first coupling step, scenario-prescribed land cover associated with any IAM
451 policy that valued carbon within unmanaged ecosystems (e.g., grassland, wetland, forest) was
452 lost. While GLM does, however, keep track internally of forested and non-forested land
453 (according to its own definition of forest, which likely differs from those within IAMs and
454 ESMs), the output land use harmonization product includes only cropland, pasture, primary, and
455 secondary land areas and transitions, and the age and biomass density of secondary land (and

456 harvest areas, carbon amounts, and transitions, which we do not address here). As each ESM
457 characterizes the land surface by its own suite of vegetation and management types (Brovkin et
458 al., 2013), additional land use and land cover information could be lost in the second coupling
459 step between GLM and the ESMs. For example, some ESMs were able to use the primary,
460 secondary, and transition information, but they might have been applying this information to
461 different land covers than those used by GLM, thus introducing a second shift away from the
462 original IAM scenario. Our specific case demonstrates an even greater inconsistency due to the
463 use of only cropland and pasture information. GCAM has 19 crop types (the CMIP5 version had
464 10) and seven managed and unmanaged land cover types while CESM has 16 PFTs, only one of
465 which is a crop type. The LUT algorithm uses only the GLM cropland and pasture area
466 information to adjust PFTs because CLM does not keep track of primary versus secondary land.
467 The resulting spatial pattern of non-crop PFTs is determined by the existing PFT distribution and
468 CESM's internal representation of potential vegetation cover (Lawrence et al., 2012;
469 Ramankutty and Foley, 1999). An additional source of error that we did not investigate here is
470 the relationship between individual PFTs and land cover types that may comprise several PFTs
471 (e.g. forest land may consist of 60% trees and 40% grass).

472 Due to the lack of a prescribed land cover input associated with the land use input, forest
473 area changes in CESM (and iESM) are effectively residual changes that are only indirectly
474 linked to GCAM forest area through changes in cropland and pasture areas. The LUT calculates
475 cropland area changes first and pasture area changes second (Figures 3 and 4). In CMIP5 CESM
476 simulations, cropland area changes cause non-crop PFTs to be added or removed in proportion to
477 their potential or existing grid-cell fractions, respectively. Pasture is more complicated because it
478 is not tracked as such: pasture is not a single PFT and its changes are represented as changes in

479 herbaceous and tree PFTs. Specifically, tree PFTs are removed when pasture is added, and non-
480 crop PFTs are added in proportion to their potential vegetation grid-cell fractions when pasture is
481 removed (Lawrence et al., 2012). This residual PFT determination, combined with independent
482 and unique forest definitions across GCAM, GLM, and CESM, causes the bulk of prescribed
483 afforestation to not appear in the CESM land surface. As a direct consequence, CESM grass area
484 (and shrub area to a lesser extent) increases while GCAM pasture decreases dramatically (Figure
485 5). CESM has this same limitation for all four RCP scenarios, and the other CMIP5 ESMs
486 implement similar inconsistencies to varying degrees due to the lack of specific vegetation types
487 in the land coupling between IAMs and ESMs. For example, Davies-Barnard et al. (2014)
488 recently reported that the HadGEM2-ES RCP4.5 forest area increased 11% from 2005-2100,
489 while the GCAM forest area increased by 24%. Additionally, the GCAM 2005 forest area was
490 41.1 Mkm², the GLM 2005 forest area was 39.9 km², but the MPI-ESM 2005 forest area was
491 about 24 M km². As a result, the 35% increase in MPI-ESM RCP4.5 forest area by 2100
492 (Wilkenskjeld et al., in review) was still only 77% of GCAM's afforestation. It is apparent from
493 these inconsistencies that interdependent land use and land cover need to be faithfully
494 transmitted from IAMs to ESMs to robustly simulate the effects of prescribed scenarios on the
495 earth system.

496 Even partial restoration of the lost afforestation signal in iESM demonstrates the
497 potentially dramatic effect on global carbon and climate of using IAM land cover and land use
498 information in ESMs. As soon as 25 years after the initial increase in forest area, and with only
499 64% of GCAM's afforestation area, the NEWLUT has a significant impact on global carbon
500 balance (Figure 9). The assumption that forest exclusively replaces abandoned cropland and
501 pasture in GCAM's land use projection (Figures 6-8) sets the upper limit for CESM because

502 there is no other information to constrain forest area, and may be applicable only to the RCP4.5
503 scenario. Although this limits NEWLUT to including only two-thirds of the total afforestation,
504 adding more forest area to CESM would be arbitrary without additional land cover information.
505 Nonetheless, the increased afforestation in NEWLUT results in an increase in net land carbon
506 uptake over the OLDLUT case due to a sustained increase in average annual land carbon uptake
507 after 2020 (Figure 9). As a result, the NEWLUT simulation increases vegetation carbon gain by
508 19 PgC and decreases atmospheric CO₂ gain by 7.7 ppmv from 2005 to 2040 in comparison to
509 OLDLUT (Figure 10). The NEWLUT simulation also decreases soil carbon gain by about 1.5
510 PgC over this period (data not shown).

511 Simple linear extrapolation of the iESM vegetation carbon gain and atmospheric CO₂
512 gain from 2005 to 2100 increases these changes to approximately 52 PgC and 21 ppmv, and
513 extending CESM forest area to match GCAM total afforestation could potentially increase these
514 changes to 88 PgC and 36 ppmv in 2100. These are rough estimates that use 2005 as a starting
515 point to reduce the high slope associated with the initial increase from 2015-2020, and also
516 assume that additional forest area continues to gain carbon for 60-80 years after it is established.
517 Regardless of the absolute accuracy of these extrapolations, the potential gain in vegetation
518 carbon alone for CESM with full afforestation is on the order of estimates of net cumulative land
519 use change emissions during 1850-2000, which range from 110-210 PgC (Table 3 in Smith and
520 Rothwell, 2013). For comparison, the range of CMIP5 vegetation carbon stock gains for RCP4.5
521 is about 50 to 300 PgC from 2005 to 2100, with most gains being less than 150 PgC and
522 relatively linear (Figure 2 in Jones et al., 2013b). An increase in gain of 88 PgC would
523 dramatically shift CESM vegetation carbon dynamics in relation to the other ESMs. The
524 corresponding 36 ppmv decrease in atmospheric CO₂ is nearly one-third of the difference

525 between the prescribed 2100 concentrations of the RCP4.5 (~540 ppmv) and RCP2.6 (~420
526 ppmv) scenarios (Figure 1 in Jones et al., 2013b). More importantly for CESM's ability to
527 robustly simulate the effects of the RCP scenarios on the earth system, the prognostic CESM
528 atmospheric CO₂ concentration in 2100 for RCP4.5 is 610 ppmv (Keppel-Aleks et al., 2013), and
529 a decrease from 610 to 574 ppmv has an approximate decrease in radiative forcing of 0.33 W m⁻
530 ², which is non-trivial with respect to the 4.5 W m⁻² target. While these carbon cycle changes in
531 the CESM component of iESM may have a significant effect on climate, it is important to note
532 that the carbon cycle effects of afforestation in CESM are not identical to those in GCAM or
533 GLM because these three models have different biogeochemistry and vegetation models. These
534 differences in carbon cycles, however, do not obviate the need for making both land cover and
535 land use consistent between IAMs and ESMs in order to best match the prescribed radiative
536 forcing scenario.

537 Different implementations of land cover and land use among IAMs and ESMs also
538 reduce the fidelity between RCP scenarios and their associated effects on the earth system.
539 Figure 8 shows that most of the additional forest area in NEWLUT occurs on grassland and
540 shrubland, and that these lands generally coincide with areas of limited potential forest. The
541 OLDLUT could not add forest area where no potential forest area exists, and the rate of forest
542 carbon accumulation is constrained by environmental conditions. GLM also limits forest area
543 and growth based on potential forest and environmental conditions, but with a different growth
544 model and map of potential forest area than used by CESM. On the other hand, GCAM
545 afforestation is a strategy to expand forest area for carbon sequestration, and assumes that it is
546 cost effective to use agricultural inputs (e.g., water, fertilizer) to achieve the expected forest
547 growth. This disagreement among the three models hampers communication of forest area

548 changes and contributes to the differences in forest area among the models, both in CMIP5
549 (Figure 5) and in the iESM (Figures 6 and 7). Nonetheless, sharing forest area between GCAM
550 and GLM does improve the fidelity between GCAM and GLM's forest area changes (Figures 5
551 and 6). GLM and CESM do not simulate agricultural inputs for forests, but the NEWLUT can
552 simulate most, but not all, of the prescribed afforestation (Figures 6 and 7) by adding forest area
553 based on GCAM's cropland and pasture changes, rather than on potential forest area. The
554 additional forest might not grow as well in CESM as in GCAM, but the CESM forest
555 productivity is fed back to GCAM for subsequent land use projections, so environmental
556 restrictions on forest growth will influence future land use and land cover. This feedback does
557 not, however, fully compensate for the lack of bioclimatic or agricultural input availability
558 constraints on GCAM's land use projection, which might contribute to an overly optimistic
559 afforestation projection. More generally, this feedback mechanism opens a path for more
560 robustly simulating interdependent land use and land cover through incorporation of potential,
561 bioclimate-driven geographic shifts in land cover. ESMs could estimate bioclimatic drivers or
562 geographic shifts for given land use/cover scenarios, and then feed this information back to the
563 IAMs for incorporation into land use/cover projection. Implementing such a feedback for
564 scenario-based simulations would consolidate land use/cover determination into internally
565 consistent modules within the IAMs, thereby increasing fidelity between the scenario-prescribed
566 land surface and the one used by the ESMs.

567 We have focused on understanding the effects of mismatched land cover areas on global
568 simulations, rather than on mismatched carbon cycles, because the spatial distribution of land
569 cover and land use is a scenario-determined boundary condition for ecosystem-specific processes
570 such as biogeochemical dynamics. For global simulations this boundary condition is generally

571 provided by historical data and IAMs, and, as we have shown, a mismatch in this boundary
572 condition causes CESM to simulate non-scenario effects on carbon and climate (due to a non-
573 scenario land surface), rather than the scenario-driven effects of the land surface prescribed for
574 meeting the RCP4.5 target. Mismatched carbon cycles among IAMs and ESMs, on the other
575 hand, along with differences in atmospheric radiation code, will preclude exact matches in
576 radiative forcing for a given RCP scenario, but should not cause significant deviations among
577 models in the carbon and climate effects of a given scenario. While we plan to completely
578 reconcile land use and land cover inconsistencies within the iESM by implementing a single
579 carbon cycle with consistent land surface characterization among the components, it is not
580 desirable, nor feasible, for all IAMs and ESMs to have the same biogeochemistry and vegetation
581 growth components. For example, a diversity of terrestrial models can help characterize
582 uncertainty in global simulations. This uncertainty, however, is most useful if these models
583 simulate the same spatial distribution of land cover and land use change. Therefore, iESM
584 redevelopment that ensures land use and land cover consistency between GCAM and CESM
585 could provide a template for improving the fidelity between IAM scenarios and ESM simulations
586 in the next CMIP. In fact, land cover information is currently planned to be included in the
587 CMIP6 land coupling, along with a more extensive land use model intercomparison project
588 (Meehl et al., 2014).

589

590 5. Conclusion

591 We have identified the lack of specific land cover type information being shared among
592 GCAM, GLM, and CESM in the iESM as the primary cause of CESM having very little
593 afforestation and effectively no change in herbaceous PFT area in contrast to GCAM's large

594 RCP4.5 afforestation and corresponding pasture reduction. Initial efforts to fix this problem
595 through GLM modifications and the sharing of forest area between GCAM and GLM improved
596 only the fidelity of forest area changes between GCAM and GLM. We then focused on
597 modifying the algorithm that translates GLM land use harmonization outputs to CESM PFTs.
598 While these land use translator modifications have been successful at capturing two-thirds of
599 GCAM's RCP4.5 afforestation signal and corresponding reductions in herbaceous PFT area,
600 they are not sufficient to completely overcome the limitations imposed by not passing specific
601 land cover types from GCAM through to CESM. These modifications are also specific to the
602 GCAM RCP4.5 scenario, and might need to be altered for the other RCP scenarios. Furthermore,
603 we have not addressed the lack of constraints on GCAM forest area expansion, nor mismatches
604 between land cover and PFT definitions. Nonetheless, this partial restoration of afforestation has
605 a significant impact on iESM's global carbon cycle through increased vegetation carbon and
606 decreased atmospheric CO₂ concentration.

607 The iESM framework follows the CMIP5 land coupling design, and as such we have
608 characterized a major gap in this design that precludes accurate translation of projected IAM land
609 surface scenarios to ESMs by focusing only on land use such as cropland and pasture (albeit
610 successfully), and not including specific land cover types such as forest, grassland, and
611 shrubland. The relationship between land use and land cover is handled uniquely by individual
612 ESMs, which means that the effects of scenario mismatch will be model-specific and more
613 relevant for some RCPs than others. The resulting land cover discrepancies are likely most
614 pronounced for the large RCP4.5 afforestation signal, which was greatly reduced in the CMIP5
615 CESM and HadGEM2-ES (see Davies-Barnard et al., 2014) simulations, but could also arise for
616 other large land cover changes such as the extensive deforestation of RCP8.5. As total land area

617 is conservative, errors in the distribution of one land cover are complemented by errors in the
618 distributions of other land covers. In GCAM's RCP4.5 scenario, pasture decreases over the 21st
619 century, but the CMIP5 CESM runs have increasing grass and shrub areas over the same period.
620 It is very important that the land use and land cover changes (which determine land use change
621 emissions and the total capacity for vegetation carbon assimilation) match between the IAMs and
622 ESMs because the CMIP5 experimental design is predicated on the fidelity between IAM
623 scenarios and ESM simulations such that they have similar, specific radiative forcings for a
624 given scenario, including CO₂ emissions from land use change (Moss et al., 2010). Furthermore,
625 future radiative climate targets are likely to include the biogeophysical forcings of land use
626 change because it has been shown that the modeled climate system is sensitive to changes in
627 these forcings due to the spatial distribution of land use and land cover change (Brovkin et al.,
628 2013; Jones et al., 2013a; Pitman et al., 2009), making it imperative that IAM and ESM land use
629 and land cover distributions match as closely as possible. Maintaining the diversity of global
630 biogeochemical and vegetation models also calls for GCMs and ESMs to match historical and
631 projected land cover and land use distributions as closely as possible, so as to isolate carbon
632 cycle contributions to uncertainty from contributions due to differences in land use and land
633 cover. Fortunately, our results indicate that it might be possible to adjust land cover in other
634 CMIP5 models to better match RCP4.5 afforestation and the corresponding climate scenario,
635 while still using the standard land use harmonization data.

636 We conclude that the land coupling between IAMs and ESMs for future model
637 intercomparisons needs to ensure greater consistency in land cover and land use among the
638 models in order to realize the full potential of scenario-based earth system simulations. In short,
639 the models need to agree on the actual land area and the annual spatial distribution of major

640 (non-) vegetation land covers and land uses. In other words, the ESMs need to simulate the same
641 basic land surface as prescribed by the IAM-generated RCP scenarios. To achieve the required
642 consistency, we suggest that the next CMIP land coupling design provides land cover and land
643 use information, and a standard mapping between land cover and plant functional types.

644 Fortunately, this is an emerging priority for the CMIP6 Land Use Model Intercomparison Project
645 (LUMIP, <http://www.wcrp-climate.org/index.php/modelling-wgcm-mip-catalogue/modelling-wgcm-mips/318-modelling-wgcm-catalogue-lumip> , http://www.wcrp-climate.org/wgcm/WGCM17/LUMIP_proposal_v4.pdf). The following gridded data with
646 fractional shares within grid cells are specifically recommended:
647

649 1) Annual land cover states with complete, contiguous spatial coverage within grid cells.

650 Land cover needs to include at least the basic categories of cropland, grassland,
651 shrubland, woodland, forest, and other (bare/sparse, ice, urban, water). This will allow
652 consistency in major (non-) vegetation types for model intercomparison (with the “other”
653 category having fixed area). The “other” categories could also be separated out for
654 models that can use them, and in preparation for changing their areas also.

655 2) Annual land use states including primary and secondary land, wood harvest, and pasture
656 (cropland should coincide with the land cover state). These uses should be provided with
657 respect to the land cover categories. Wood harvest and pasture should include both area
658 and amount of biomass/carbon harvested or removed by grazing.

659 3) A standard present-day land area data set to be used by all models. Land area includes all
660 land cover and land use categories as described above.

661 4) Annual land use and land cover transitions. Land use transitions need to be accompanied
662 by corresponding land cover transitions with complete, contiguous spatial coverage

663 within grid cells. Net land use/cover transitions, which should be used for model
664 intercomparison, are annual changes in individual land use and cover states, and may
665 include additional detail about sources of wood harvest and grazed biomass. Gross land
666 use/cover transitions are the transitions among particular land use/covers occurring within
667 a particular year. These transitions sum to the net land use/cover transitions, and should
668 also be provided to characterize shifting cultivation and other gross land conversions.
669 While gross land use/cover transitions are very important and make a significant
670 difference in the carbon cycle, until more models are able to make use of gross transitions
671 they should not be included in model intercomparisons.

672

673 Acknowledgements

674 We are extremely grateful to Peter Lawrence (National Center for Atmospheric
675 Research) for providing the original CESM land use translation code. This material is based
676 upon work supported by the U.S. Department of Energy, Office of Science, Office of Biological
677 and Environmental Research under Award Number DE-AC02-05CH11231 as part of the
678 Integrated Assessment Research and Earth System Modeling Programs. This project used
679 resources of the National Energy Research Scientific Computing Center (NERSC), which is a
680 DOE Office of Science User Facility. The CESM project is supported by the National Science
681 Foundation and the Office of Science (Biological and Environmental Research) of the U.S.
682 Department of Energy. We also gratefully acknowledge the support of the National Aeronautics
683 and Space Administration.

685 References

686 Adegoke, J. O., Pielke Sr, R., and Carleton, A. M.: Observational and modeling studies of the
 687 impacts of agriculture-related land use change on planetary boundary layer processes in
 688 the central u.S, Agricultural and Forest Meteorology, 142, 203-215,
 689 <http://dx.doi.org/10.1016/j.agrformet.2006.07.013>, 2007.

690 Anav, A., Friedlingstein, P., Kidston, M., Bopp, L., Ciais, P., Cox, P., Jones, C., Jung, M.,
 691 Myneni, R., and Zhu, Z.: Evaluating the land and ocean components of the global carbon
 692 cycle in the cmip5 earth system models, J. Clim., 26, 6801-6843, 10.1175/jcli-d-12-
 693 00417.1, 2013.

694 Arora, V. K., and Boer, G. J.: Uncertainties in the 20th century carbon budget associated with
 695 land use change, Global Change Biol., 16, 3327-3348, 10.1111/j.1365-
 696 2486.2010.02202.x, 2010.

697 Baidya Roy, S., Hurtt, G. C., Weaver, C. P., and Pacala, S. W.: Impact of historical land cover
 698 change on the july climate of the united states, Journal of Geophysical Research:
 699 Atmospheres, 108, 4793, 10.1029/2003jd003565, 2003.

700 Bitz, C. M., Shell, K. M., Gent, P. R., Bailey, D. A., Danabasoglu, G., Armour, K. C., Holland,
 701 M. M., and Kiehl, J. T.: Climate sensitivity of the community climate system model,
 702 version 4, J. Clim., 25, 3053-3070, 10.1175/jcli-d-11-00290.1, 2011.

703 Bond-Lamberty, B., Calvin, K., Jones, A. D., Mao, J., Patel, P., Shi, X., Thomson, A., Thornton,
 704 P., and Zhou, Y.: Coupling earth system and integrated assessment models: the problem
 705 of steady state, Geoscientific Model Development Discuss, 7, 1499-1524, doi:
 706 10.5194/gmdd-7-1499-2014, 2014.

707 Brovkin, V., Boysen, L., Arora, V. K., Boisier, J. P., Cadule, P., Chini, L., Claussen, M.,
 708 Friedlingstein, P., Gayler, V., van den Hurk, B. J. J. M., Hurtt, G. C., Jones, C. D., Kato,
 709 E., de Noblet-Ducoudré, N., Pacifico, F., Pongratz, J., and Weiss, M.: Effect of
 710 anthropogenic land-use and land-cover changes on climate and land carbon storage in
 711 cmip5 projections for the twenty-first century, J. Clim., 26, 6859-6881, 10.1175/jcli-d-
 712 12-00623.1, 2013.

713 Calvin K., Clarke, L. E., Edmonds, J. A., Eom, J., Hejazi, M. I., Kim, S. H., Kyle, G. P., Link, R.
 714 P., Luckow, P., Patel, P. L., Smith, S. J., and Wise, M. A.: GCAM Wiki Documentation,
 715 PNNL-20809, Pacific Northwest National Laboratory, Richland, WA,
 716 <http://wiki.umd.edu/gcam/>, 2011.

717 Davies-Barnard, T., Valdes, P. J., Singarayer, J. S., and Jones, C. D.: Climatic impacts of land-
 718 use change due to crop yield increases and a universal carbon tax from a scenario model,
 719 J. Clim., 27, 1413-1424, 10.1175/jcli-d-13-00154.1, 2014.

720 Friedlingstein, P., Cox, P., Betts, R., Bopp, L., von Bloh, W., Brovkin, V., Cadule, P., Doney, S.,
 721 Eby, M., Fung, I., Bala, G., John, J., Jones, C., Joos, F., Kato, T., Kawamiya, M., Knorr,
 722 W., Lindsay, K., Matthews, H. D., Raddatz, T., Rayner, P., Reick, C., Roeckner, E.,
 723 Schnitzler, K.-G., Schnur, R., Strassmann, K., Weaver, A. J., Yoshikawa, C., and Zeng,
 724 N.: Climate-carbon cycle feedback analysis: Results from the c4mip model
 725 intercomparison, J. Clim., 19, 3337-3353, doi:10.1175/JCLI3800.1, 2006.

726 Gent, P. R., Danabasoglu, G., Donner, L. J., Holland, M. M., Hunke, E. C., Jayne, S. R.,
 727 Lawrence, D. M., Neale, R. B., Rasch, P. J., Vertenstein, M., Worley, P. H., Yang, Z.-L.,

728 and Zhang, M.: The community climate system model version 4, *J. Clim.*, 24, 4973-4991,
 729 10.1175/2011jcli4083.1, 2011.

730 Houghton, R. A.: How well do we know the flux of co 2 from land-use change?, *Tellus B*, 62(5),
 731 337-351, doi: 10.1111/j.1600-0889.2010.00473.x, 2010.

732 Houghton, R. A., House, J. I., Pongratz, J., van der Werf, G. R., DeFries, R. S., Hansen, M. C.,
 733 Le Quere, C., and Ramankutty, N.: Carbon emissions from land use and land-cover
 734 change, *Biogeosciences*, 9, 5125-5142, 10.5194/bg-9-5125-2012, 2012.

735 Hurtt, G. C., Pacala, S. W., Moorcroft, P. R., Caspersen, J., Shevliakova, E., Houghton, R. A.,
 736 and Moore, B.: Projecting the future of the u.S. Carbon sink, *Proceedings of the National
 737 Academy of Sciences*, 99, 1389-1394, 10.1073/pnas.012249999, 2002.

738 Hurtt, G. C., Frolking, S., Fearon, M. G., Moore, B., Shevliakova, E., Malyshev, S., Pacala, S.
 739 W., and Houghton, R. A.: The underpinnings of land-use history: Three centuries of
 740 global gridded land-use transitions, wood-harvest activity, and resulting secondary lands,
 741 *Global Change Biol.*, 12, 1208-1229, 10.1111/j.1365-2486.2006.01150.x, 2006.

742 Hurtt, G. C., Chini, L. P., Frolking, S., Betts, R. A., Feddema, J., Fischer, G., Fisk, J. P.,
 743 Hibbard, K., Houghton, R. A., Janetos, A., Jones, C. D., Kindermann, G., Kinoshita, T.,
 744 Klein Goldewijk, K., Riahi, K., Shevliakova, E., Smith, S., Stehfest, E., Thomson, A.,
 745 Thornton, P., Vuuren, D. P., and Wang, Y. P.: Harmonization of land-use scenarios for
 746 the period 1500-2100: 600 years of global gridded annual land-use transitions, wood
 747 harvest, and resulting secondary lands, *Clim. Change*, 109, 117-161, 10.1007/s10584-
 748 011-0153-2, 2011.

749 Jain, A. K., and Yang, X.: Modeling the effects of two different land cover change data sets on
 750 the carbon stocks of plants and soils in concert with co2 and climate change, *Global
 751 Biogeochemical Cycles*, 19, GB2015, 10.1029/2004gb002349, 2005.

752 Jain, A. K., Meiyappan, P., Song, Y., and House, J. I.: Co2 emissions from land-use change
 753 affected more by nitrogen cycle, than by the choice of land-cover data, *Global Change
 754 Biol.*, 19, 2893-2906, 10.1111/gcb.12207, 2013.

755 Jones, A. D., Collins, W. D., Edmonds, J., Torn, M. S., Janetos, A., Calvin, K. V., Thomson, A.,
 756 Chini, L. P., Mao, J., Shi, X., Thornton, P., Hurtt, G. C., and Wise, M.: Greenhouse gas
 757 policy influences climate via direct effects of land-use change, *J. Clim.*, 26, 3657-3670,
 758 10.1175/jcli-d-12-00377.1, 2013a.

759 Jones, C. D., Hughes, J. K., Bellouin, N., Hardiman, S. C., Jones, G. S., Knight, J., Liddicoat, S.,
 760 O'Connor, F. M., Andres, R. J., Bell, C., Boo, K.-O., Bozzo, A., Butchart, N., Cadule, P.,
 761 Corbin, K. D., Doutriaux-Boucher, M., Friedlingstein, P., Gornall, J., Gray, L.,
 762 Halloran, P. R., Hurtt, G., Ingram, W. J., Lamarque, J.-F., Law, R. M., Meinshausen, M.,
 763 Osprey, S., Palin, E. J., Parsons Chini, L., Raddatz, T., Sanderson, M. G., Sellar, A. A.,
 764 Schurer, A., Valdes, P., Wood, N., Woodward, S., Yoshioka, M., and Zerroukat, M.: The
 765 HadGEM2-ES implementation of CMIP5 centennial simulations, *Geosci. Model Dev.*, 4,
 766 543-570, doi:10.5194/gmd-4-543-2011, 2011.

767 Jones, C., Robertson, E., Arora, V., Friedlingstein, P., Shevliakova, E., Bopp, L., Brovkin, V.,
 768 Hajima, T., Kato, E., Kawamiya, M., Liddicoat, S., Lindsay, K., Reick, C. H., Roelandt,
 769 C., Segschneider, J., and Tjiputra, J.: Twenty-first-century compatible co2 emissions and
 770 airborne fraction simulated by cmip5 earth system models under four representative
 771 concentration pathways, *J. Clim.*, 26, 4398-4413, 10.1175/jcli-d-12-00554.1, 2013b.

772 Keppel-Aleks, G., Randerson, J. T., Lindsay, K., Stephens, B. B., Moore, J. K., Doney, S. C.,
 773 Thornton, P. E., Mahowald, N. M., Hoffman, F. M., Sweeney, C., Tans, P. P., Wennberg,

774 P. O., and Wofsy, S. C.: Atmospheric Carbon Dioxide Variability in the Community
 775 Earth System Model: Evaluation and Transient Dynamics during the Twentieth and
 776 Twenty-First Centuries, *J. Clim.*, 26, 4447-4475, 10.1175/jcli-d-12-00589.1, 2013.

777 Klein Goldewijk, K., Beusen, A., van Drecht, G., and de Vos, M.: The hyde 3.1 spatially explicit
 778 database of human-induced global land-use change over the past 12,000 years, *Global*
 779 *Ecol. Biogeogr.*, 20, 73-86, 10.1111/j.1466-8238.2010.00587.x, 2011.

780 Kyle, G. P., Luckow, P., Calvin, K., Emanuel, W., Nathan, M., and Zhou, Y.: Gcam 3.0
 781 agriculture and land use: Data sources and methods, *Pacific Northwest National*
 782 *Laboratory*, 58, 2011.

783 Lawrence, D. M., Oleson, K. W., Flanner, M. G., Thornton, P. E., Swenson, S. C., Lawrence, P.
 784 J., Zeng, X., Yang, Z.-L., Levis, S., Sakaguchi, K., Bonan, G. B., and Slater, A. G.:
 785 Parameterization improvements and functional and structural advances in version 4 of the
 786 community land model, *Journal of Advances in Modeling Earth Systems*, 3, M03001,
 787 10.1029/2011ms000045, 2011.

788 Lawrence, P. J., Feddema, J. J., Bonan, G. B., Meehl, G. A., O'Neill, B. C., Oleson, K. W.,
 789 Levis, S., Lawrence, D. M., Kluzek, E., Lindsay, K., and Thornton, P. E.: Simulating the
 790 biogeochemical and biogeophysical impacts of transient land cover change and wood
 791 harvest in the community climate system model (ccsm4) from 1850 to 2100, *J. Clim.*, 25,
 792 3071-3095, 10.1175/jcli-d-11-00256.1, 2012.

793 Lee, H.-L., Hertel, T. W., Sohngen, B., and Ramankutty, N.: Towards an integrated land use
 794 database for assessing the potential for greenhouse gas mitigation, *Purdue University*, 83,
 795 2005.

796 Masui, T., Matsumoto, K., Hijioka, Y., Kinoshita, T., Nozawa, T., Ishiwatari, S., Kato, E.,
 797 Shukla, P. R., Yamagata, Y., and Kainuma, M.: An emission pathway for stabilization at
 798 6 Wm² radiative forcing, *Clim. Change*, 109, 59-76, 10.1007/s10584-011-0150-5, 2011.

799 Meehl, G. A., Moss, R., Taylor, K. E., Eyring, V., Stouffer, R. J., Bony, S., and Stevens, B.:
 800 Climate model intercomparisons: Preparing for the next phase, *EOS Trans. Am.*
 801 *Geophys. Union*, 95, 77-84, 2014.

802 Moss, R. H., Edmonds, J. A., Hibbard, K. A., Manning, M. R., Rose, S. K., van Vuuren, D. P.,
 803 Carter, T. R., Emori, S., Kainuma, M., Kram, T., Meehl, G. A., Mitchell, J. F. B.,
 804 Nakicenovic, N., Riahi, K., Smith, S. J., Stouffer, R. J., Thomson, A. M., Weyant, J. P.,
 805 and Wilbanks, T. J.: The next generation of scenarios for climate change research and
 806 assessment, *Nature*, 463, 747-756, doi: 10.1038/nature08823, 2010.

807 Pitman, A. J., de Noblet-Ducoudré, N., Cruz, F. T., Davin, E. L., Bonan, G. B., Brovkin, V.,
 808 Claussen, M., Delire, C., Ganzeveld, L., Gayler, V., van den Hurk, B. J. J. M., Lawrence,
 809 P. J., van der Molen, M. K., Müller, C., Reick, C. H., Seneviratne, S. I., Strengers, B. J.,
 810 and Volodire, A.: Uncertainties in climate responses to past land cover change: First
 811 results from the lucid intercomparison study, *Geophys. Res. Lett.*, 36, L14814,
 812 10.1029/2009gl039076, 2009.

813 Raddatz, R. L.: Evidence for the influence of agriculture on weather and climate through the
 814 transformation and management of vegetation: Illustrated by examples from the canadian
 815 prairies, *Agricultural and Forest Meteorology*, 142, 186-202,
 816 <http://dx.doi.org/10.1016/j.agrformet.2006.08.022>, 2007.

817 Ramankutty, N., and Foley, J. A.: Estimating historical changes in global land cover: Croplands
 818 from 1700 to 1992, *Global Biogeochem. Cycles*, 13, 997-1027, 10.1029/1999gb900046,
 819 1999.

820 Reilly, J., Melillo, J., Cai, Y., Kicklighter, D., Gurgel, A., Paltsev, S., Cronin, T., Sokolov, A.,
821 and Schlosser, A.: Using land to mitigate climate change: Hitting the target, recognizing
822 the trade-offs, *Environ. Sci. Technol.*, 46, 5672-5679, 10.1021/es2034729, 2012.

823 Riahi, K., Rao, S., Krey, V., Cho, C., Chirkov, V., Fischer, G., Kindermann, G., Nakicenovic,
824 N., and Rafaj, P.: Rcp 8.5--a scenario of comparatively high greenhouse gas emissions,
825 *Clim. Change*, 109, 33-57, 10.1007/s10584-011-0149-y, 2011.

826 Rose, S. K., Ahammad, H., Eickhout, B., Fisher, B., Kurosawa, A., Rao, S., Riahi, K., and van
827 Vuuren, D. P.: Land-based mitigation in climate stabilization, *Energy Economics*, 34,
828 365-380, 10.1016/j.eneco.2011.06.004, 2012.

829 Shevliakova, E., Pacala, S. W., Malyshev, S., Hurtt, G. C., Milly, P. C. D., Caspersen, J. P.,
830 Sentman, L. T., Fisk, J. P., Wirth, C., and Crevoisier, C.: Carbon cycling under 300 years
831 of land use change: Importance of the secondary vegetation sink, *Global Biogeochemical
832 Cycles*, 23, GB2022, 10.1029/2007gb003176, 2009.

833 Shevliakova, E., Stouffer, R. J., Malyshev, S., Krasting, J. P., Hurtt, G. C., and Pacala, S. W.:
834 Historical warming reduced due to enhance land carbon uptake, *PNAS*, 110, 16730-
835 16735, 10.1073/pnas.1314047110, 2013.

836 Smith, P., Haberl, H., Popp, A., Erb, K.-h., Lauk, C., Harper, R., Tubiello, F. N., de Siqueira
837 Pinto, A., Jafari, M., Sohi, S., Masera, O., Böttcher, H., Berndes, G., Bustamante, M.,
838 Ahammad, H., Clark, H., Dong, H., Elsiddig, E. A., Mbow, C., Ravindranath, N. H.,
839 Rice, C. W., Robledo Abad, C., Romanovskaya, A., Sperling, F., Herrero, M., House, J.
840 I., and Rose, S.: How much land-based greenhouse gas mitigation can be achieved
841 without compromising food security and environmental goals?, *Global Change Biol.*, 19,
842 2285-2302, 10.1111/gcb.12160, 2013a.

843 Smith, R., Jones, P., Briegleb, B., Bryan, F., Danabasoglu, G., Dennis, J., Dukowicz, J., Eden,
844 C., Fox-Kemper, B., Gent, P., Hecht, M., Jayne, S., Jochum, M., Large, W., Lindsay, K.,
845 Maltrud, M., Norton, N., Peacock, S., Vertenstein, M., and Yeager, S.: The parallel ocean
846 program (pop) reference manual, Los Alamos National Laboratory, 183, 2013b.

847 Smith, S. J., and Rothwell, A.: Carbon density and anthropogenic land-use influences on net
848 land-use change emissions, *Biogeosciences*, 10, 6323-6337, 10.5194/bg-10-6323-2013,
849 2013.

850 Taylor, K. E., Stouffer, R. J., and Meehl, G. A.: An overview of cmip5 and the experiment
851 design, *Bulletin of the American Meteorological Society*, 93, 485-498, 10.1175/bams-d-
852 11-00094.1, 2012.

853 Thomson, A., Calvin, K., Smith, S., Kyle, G. P., Volke, A., Patel, P., Delgado-Arias, S., Bond-
854 Lamberty, B., Wise, M., Clarke, L., and Edmonds, J.: Rcp4.5: A pathway for stabilization
855 of radiative forcing by 2100, *Clim. Change*, 109, 77-94, 10.1007/s10584-011-0151-4,
856 2011.

857 Thornton, P. E., Lamarque, J.-F., Rosenbloom, N. A., and Mahowald, N. M.: Influence of
858 carbon-nitrogen cycle coupling on land model response to CO₂ fertilization and climate
859 variability, *Global Biogeochemical Cycles*, 21, GB4018, 10.1029/2006gb002868, 2007.

860 van Vuuren, D., Edmonds, J., Kainuma, M., Riahi, K., Thomson, A., Hibbard, K., Hurtt, G.,
861 Kram, T., Krey, V., Lamarque, J.-F., Masui, T., Meinshausen, M., Nakicenovic, N.,
862 Smith, S., and Rose, S.: The representative concentration pathways: An overview, *Clim.
863 Change*, 109, 5-31, 10.1007/s10584-011-0148-z, 2011a.

864 van Vuuren, D., Stehfest, E., Elzen, M. J., Kram, T., Vliet, J., Deetman, S., Isaac, M., Klein
865 Goldewijk, K., Hof, A., Mendoza Beltran, A., Oostenrijk, R., and Ruijven, B.: Rcp2.6:

866 Exploring the possibility to keep global mean temperature increase below 2°C, Clim.
867 Change, 109, 95-116, 10.1007/s10584-011-0152-3, 2011b.

868 Wilkenskjeld, S., Kloster, S., Pongratz, J., Raddatz, T., and Reick, C.: Comparing the influence
869 of net and gross anthropogenic land use and land cover changes on the carbon cycle in
870 the MPI-ESM, Biogeosciences Discuss., 11, 5443-5469, 10.5194/bgd-11-5443-2014,
871 2014.

872 Wise, M., Calvin, K., Thomson, A., Clarke, L., Bond-Lamberty, B., Sands, R., Smith, S. J.,
873 Janetos, A., and Edmonds, J.: Implications of limiting CO₂ concentrations for land use
874 and energy, Science, 324, 1183-1186, 10.1126/science.1168475, 2009.

875 Wise, M., and Calvin, K.: Gcam 3.0 agriculture and land use: Technical description of modeling
876 approach, Pacific Northwest National Laboratory, 51, 2011.

877

878
879 Figure captions
880
881 Figure 1. Implementation of integrated Earth System Model (iESM) terrestrial feedbacks. The
882 light blue arrows show information flow from GCAM to CESM. The light green arrows show
883 information flow from CESM to GCAM. The dashed gray outline, including the arrow crossed
884 out by green, represents the CMIP5 land coupling. The solid green outline, minus the arrow
885 crossed out by green, depicts the iESM implementation used in this study. GCAM: Global
886 Change Assessment Model. GLM: Global Land use Model. CESM: Community Earth System
887 Model.
888
889 Figure 2. General integrated Earth System Model (iESM) land use coupling algorithm. Forest
890 area is not passed from the Global Change Assessment Model (GCAM) to the Global Land use
891 Model (GLM) in the CMIP5 land use coupling, but it is passed in the iESM simulations used in
892 this study. NPP: Net Primary Productivity. HR: Heterotrophic Respiration. PFT: Plant Functional
893 Type.
894
895 Figure 3. OLD Land Use Translator (OLDLUT) algorithm for dynamic Plant Functional Type
896 (PFT) coverage. When cropland and pasture decrease, non-crop PFTs are added in proportion to
897 potential vegetation fractions. When cropland and pasture increase, non-crop PFTs are removed
898 in proportion to reference year fractions.
899
900 Figure 4. NEW Land Use Translator (NEWLUT) algorithm for dynamic Plant Functional Type
901 (PFT) coverage. When cropland and pasture decrease, tree PFTs are added in proportion to

902 potential vegetation fractions. When cropland and pasture increase, tree PFTs are removed first,
903 then other non-crop PFTs, in proportion to reference year fractions.

904
905 Figure 5. Projected global forest, pasture, grass, and shrub areas for the CMIP5 4.5 W m⁻²
906 Representative Concentration Pathway (RCP4.5), in million km². CESM: Community Earth
907 System Model. GLM: Global Land use Model. PFT: Plant Functional Type.

908
909 Figure 6. Integrated Earth System Model (iESM) land use and forest area changes with respect to
910 2015. The GLM-NEWLUT forest and pasture data are nearly identical to the GLM-OLDLUT
911 data and are not shown for clarity. Similarly, the GLM-NEWLUT cropland data are nearly
912 identical to the GCAM-NEWLUT data. CESM: Community Earth System Model. GCAM:
913 Global Change Assessment Model. GLM: Global Land use Model.

914
915 Figure 7. Integrated Earth System Model (iESM) land use and forest area. The GLM-NEWLUT
916 forest and pasture data are nearly identical to the GLM-OLDLUT data and are not shown for
917 clarity. Similarly, the GLM-NEWLUT cropland data track the GCAM-NEWLUT data, but with
918 the same offset as for the GLM-OLDLUT data. CESM: Community Earth System Model.
919 GCAM: Global Change Assessment Model. GLM: Global Land use Model.

920
921 Figure 8. Spatial distributions of iESM increased forest Plant Functional Types (PFTs),
922 decreased grass and shrub PFTs, and potential forest PFTs, as percentages of land area within
923 each grid cell. a) Difference in 2040 forest PFT area (NEWLUT - OLDLUT). b) Difference in
924 2040 grass plus shrub PFT area (NEWLUT - OLDLUT). c) Potential forest PFT area.

925
926 Figure 9. Net Ecosystem Exchange (NEE) comparison between iESM simulations. a) NEE for
927 each simulation. b) NEE difference (NEWLUT minus OLDLUT). These data show more land

928 carbon uptake (negative NEE), associated with the additional trees, for the NEWLUT simulation
929 during the afforestation period (2015 forward).

930
931 Figure 10. Comparison between iESM simulations of a-b) vegetation carbon and c-d)
932 atmospheric CO₂ concentration. Differences are NEWLUT minus OLDLUT. Due to additional
933 forest area, the NEWLUT simulation significantly increases vegetation carbon gain and
934 decreases atmospheric CO₂ gain over the OLDLUT simulation.

935
936

937

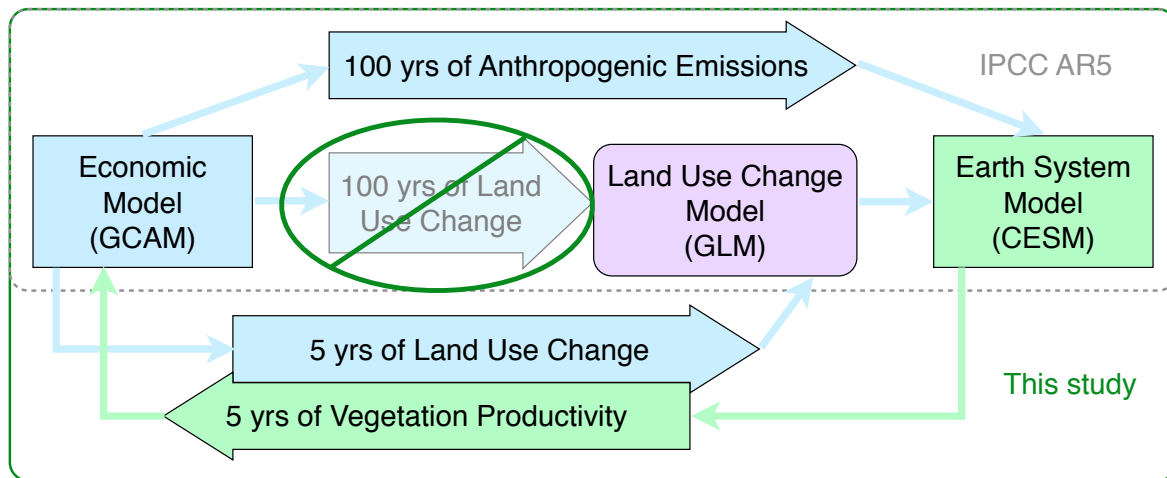
938 Table 1. Two integrated Earth System Model (iESM) simulations performed for this study.

	OLDLUT	NEWLUT
Modified Land Use Translator	N	Y
Vegetation productivity feedbacks	Y	Y
Updated Global Land use Model	Y	Y

939

940

941



942

943

Figure 1. [Implementation of integrated Earth System Model \(iESM\) terrestrial feedbacks](#).

944

The light blue arrows show information flow from GCAM to CESM. The light green arrows

945

show information flow from CESM to GCAM. The dashed gray outline, including the [arrow](#)

946

[crossed out by green](#), represents the CMIP5 land coupling. The solid green outline, minus the

947

arrow crossed out by green, depicts the iESM implementation [used in this study](#). GCAM: Global

948

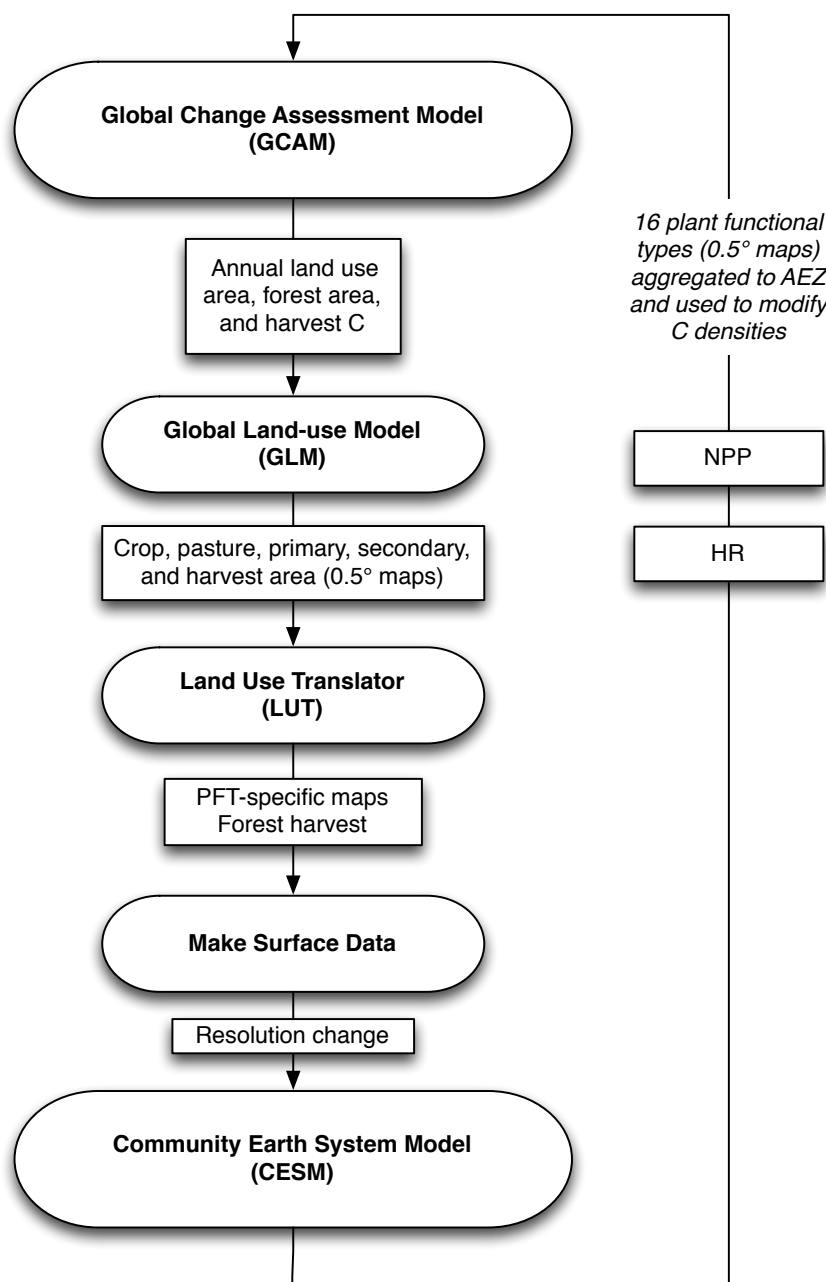
Change Assessment Model. GLM: Global Land use Model. CESM: Community Earth System

949

Model.

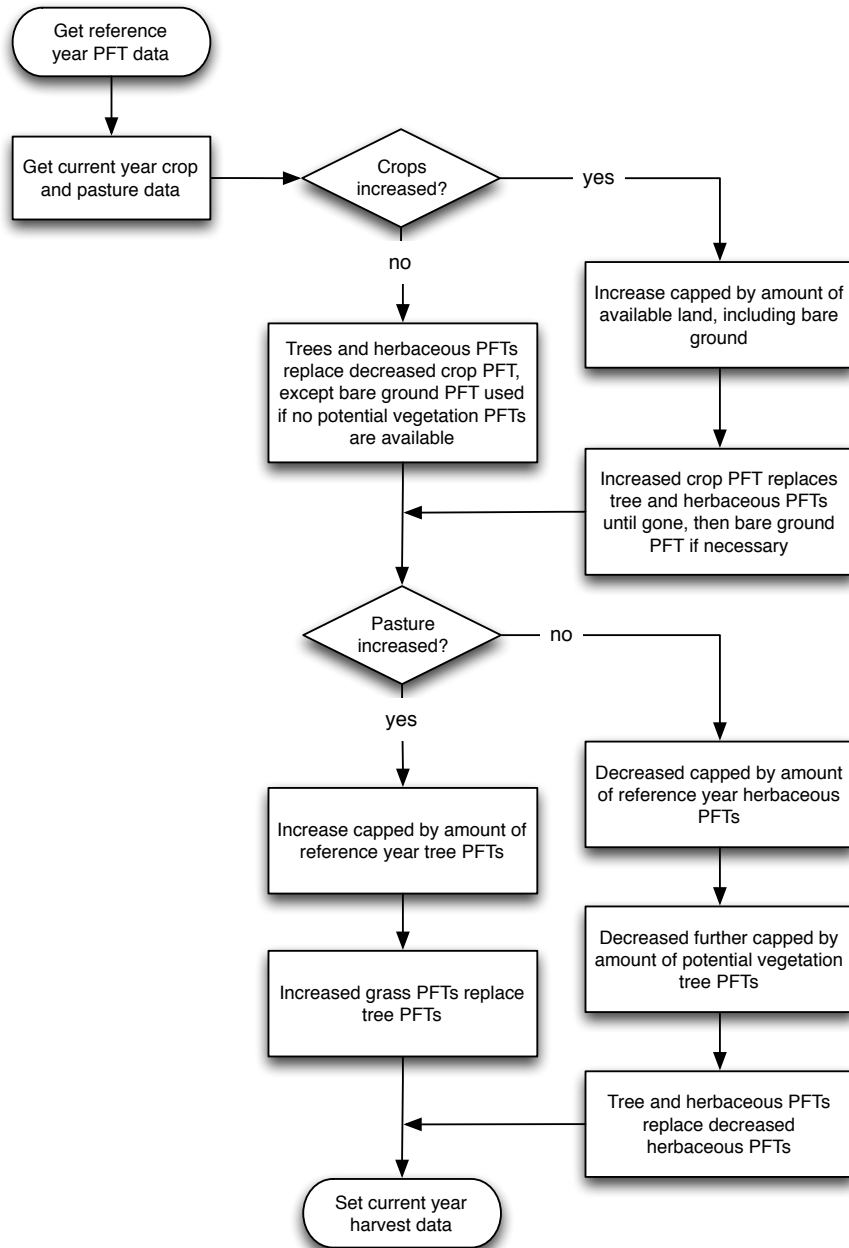
950

951



952

953 Figure 2. General integrated Earth System Model (iESM) land use coupling algorithm. Forest
954 area is not passed from the Global Change Assessment Model (GCAM) to the Global Land use
955 Model (GLM) in the CMIP5 land use coupling, but it is passed in the iESM simulations used in
956 this study. NPP: Net Primary Productivity. HR: Heterotrophic Respiration. PFT: Plant Functional
957 Type.

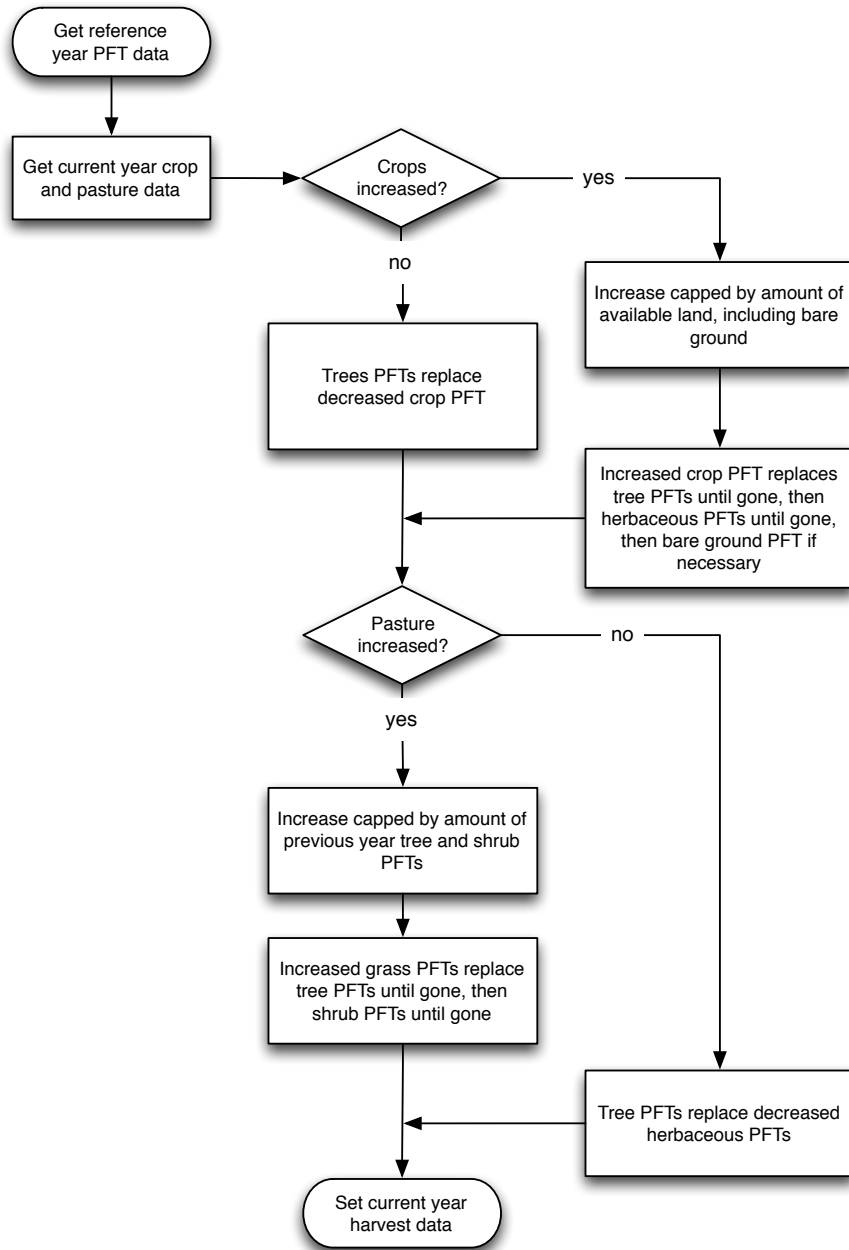


958

959 Figure 3. OLD Land Use Translator (OLDLUT) algorithm for dynamic Plant Functional Type
 960 (PFT) coverage. When cropland and pasture decrease, non-crop PFTs are added in proportion to
 961 potential vegetation fractions. When cropland and pasture increase, non-crop PFTs are removed
 962 in proportion to reference year fractions.

963

964

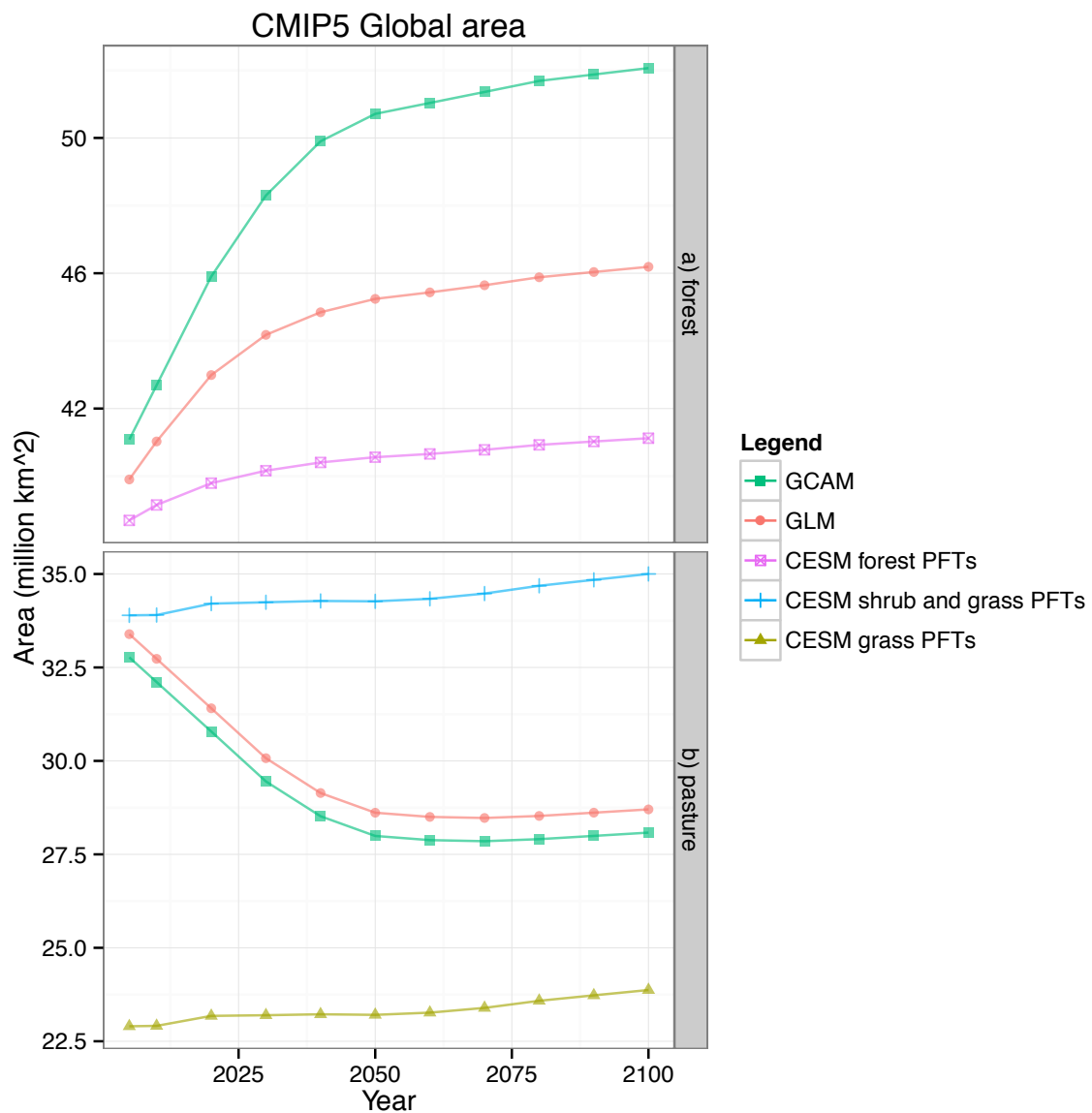


965

966 Figure 4. NEW Land Use Translator (NEWLUT) algorithm for dynamic Plant Functional Type
 967 (PFT) coverage. When cropland and pasture decrease, tree PFTs are added in proportion to
 968 potential vegetation fractions. When cropland and pasture increase, tree PFTs are removed first,
 969 then other non-crop PFTs, in proportion to reference year fractions.

970

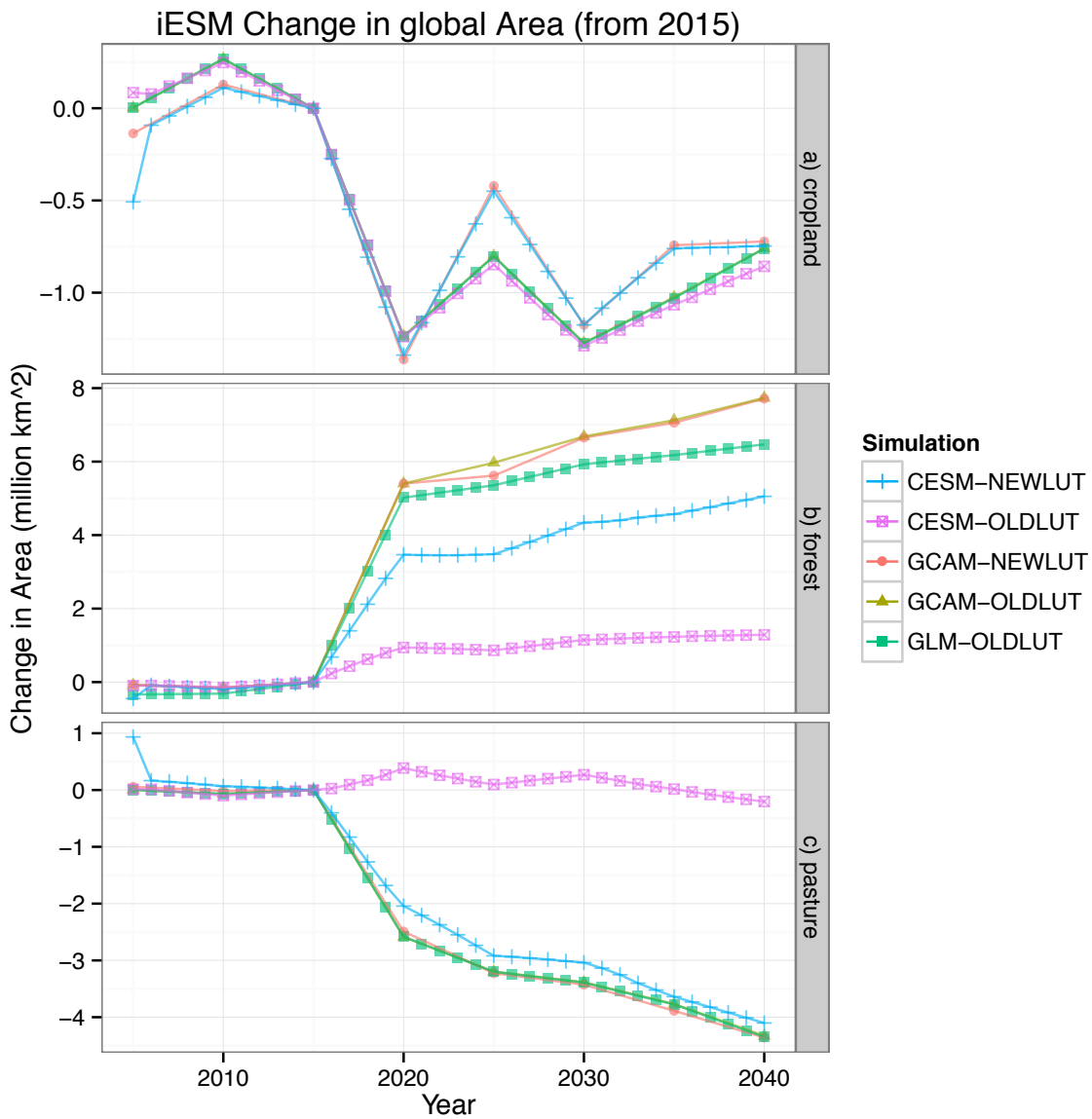
971



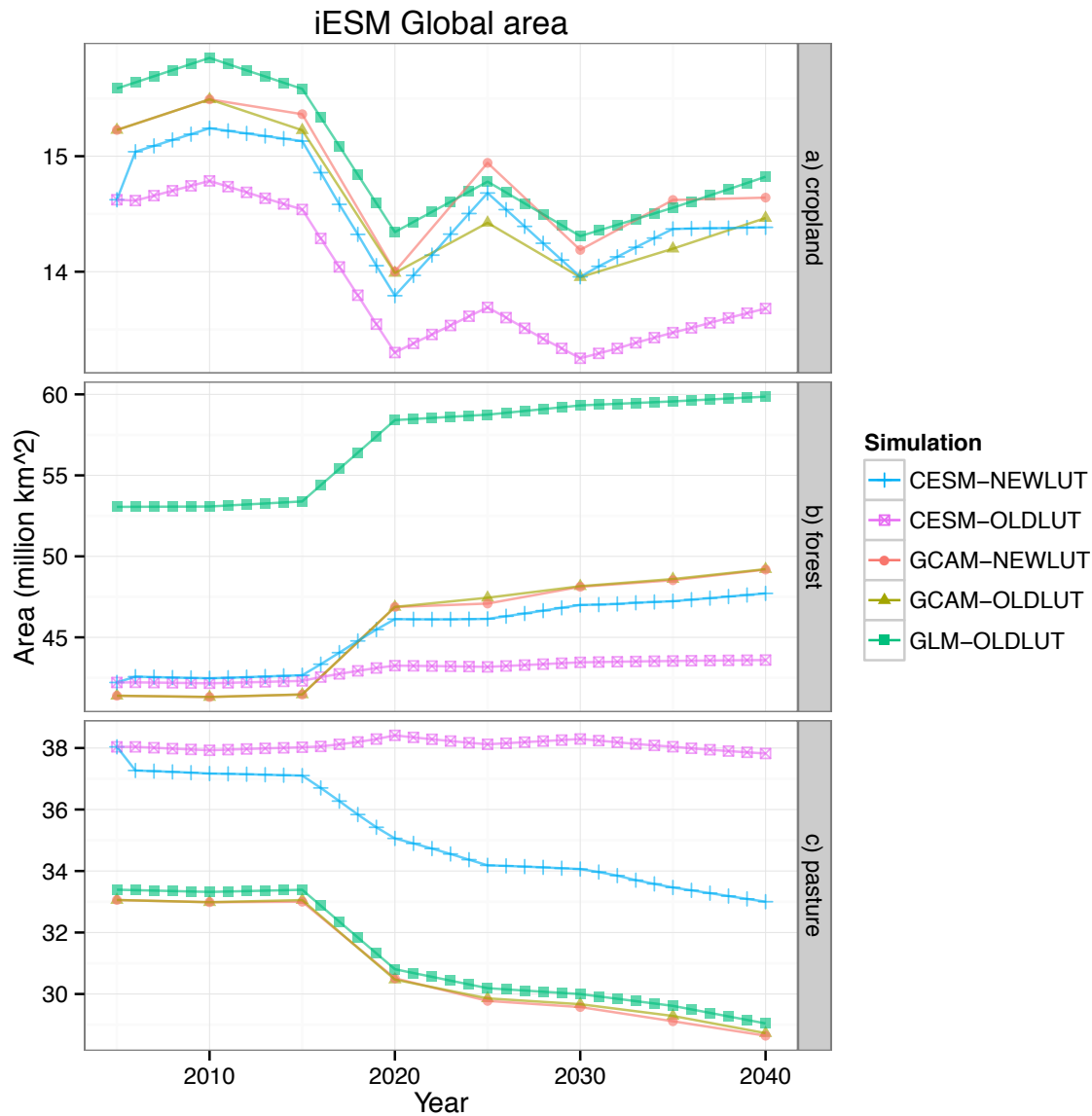
972

973 Figure 5. Projected global forest, pasture, grass, and shrub areas for the CMIP5 4.5 W m^{-2}
974 Representative Concentration Pathway (RCP4.5), in million km^2 . CESM: Community Earth
975 System Model. GLM: Global Land use Model. PFT: Plant Functional Type.

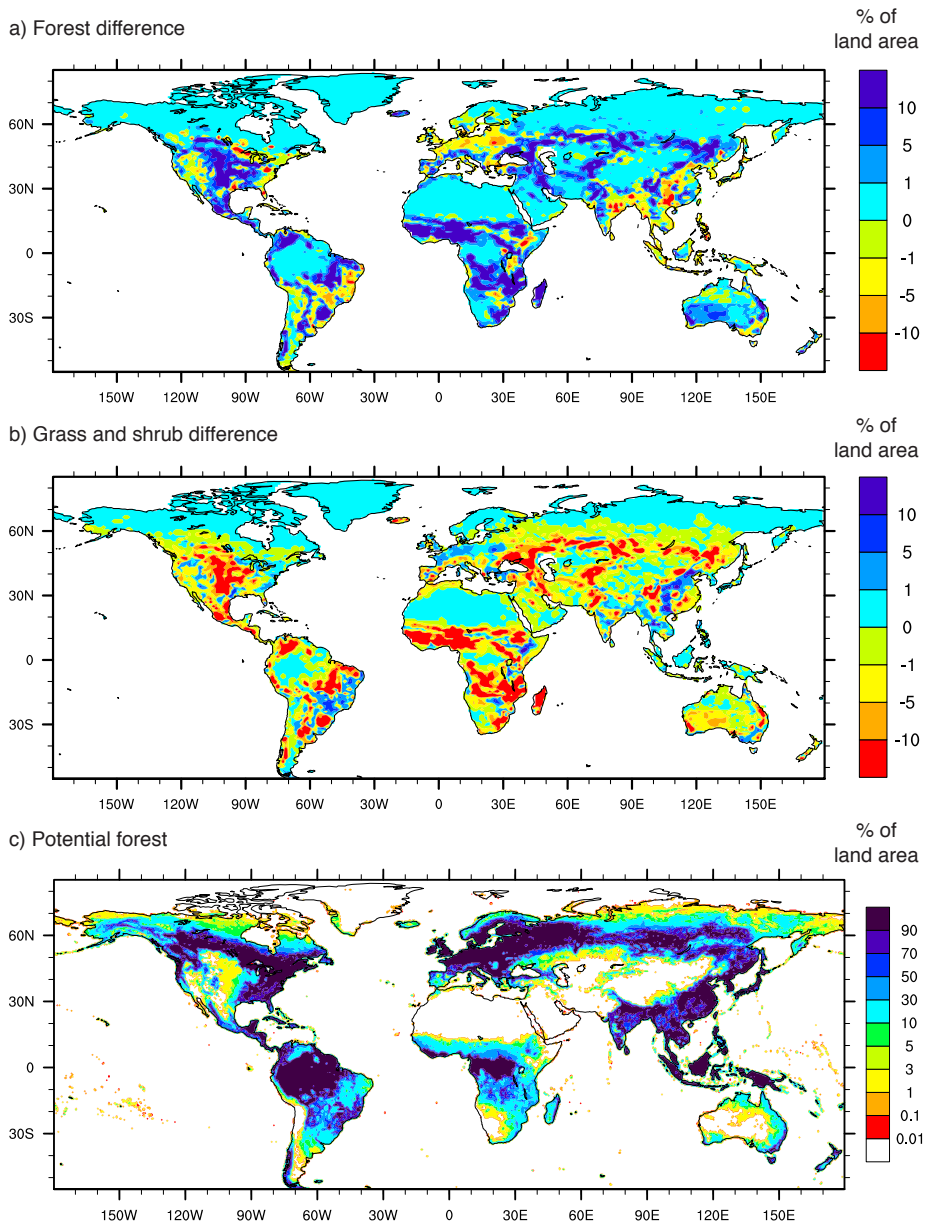
976



979 Figure 6. Integrated Earth System Model (iESM) land use and forest area changes with respect to
 980 2015. The GLM-NEWLUT forest and pasture data are nearly identical to the GLM-OLDLUT
 981 data and are not shown for clarity. Similarly, the GLM-NEWLUT cropland data are nearly
 982 identical to the GCAM-NEWLUT data. CESM: Community Earth System Model. GCAM:
 983 Global Change Assessment Model. GLM: Global Land use Model.

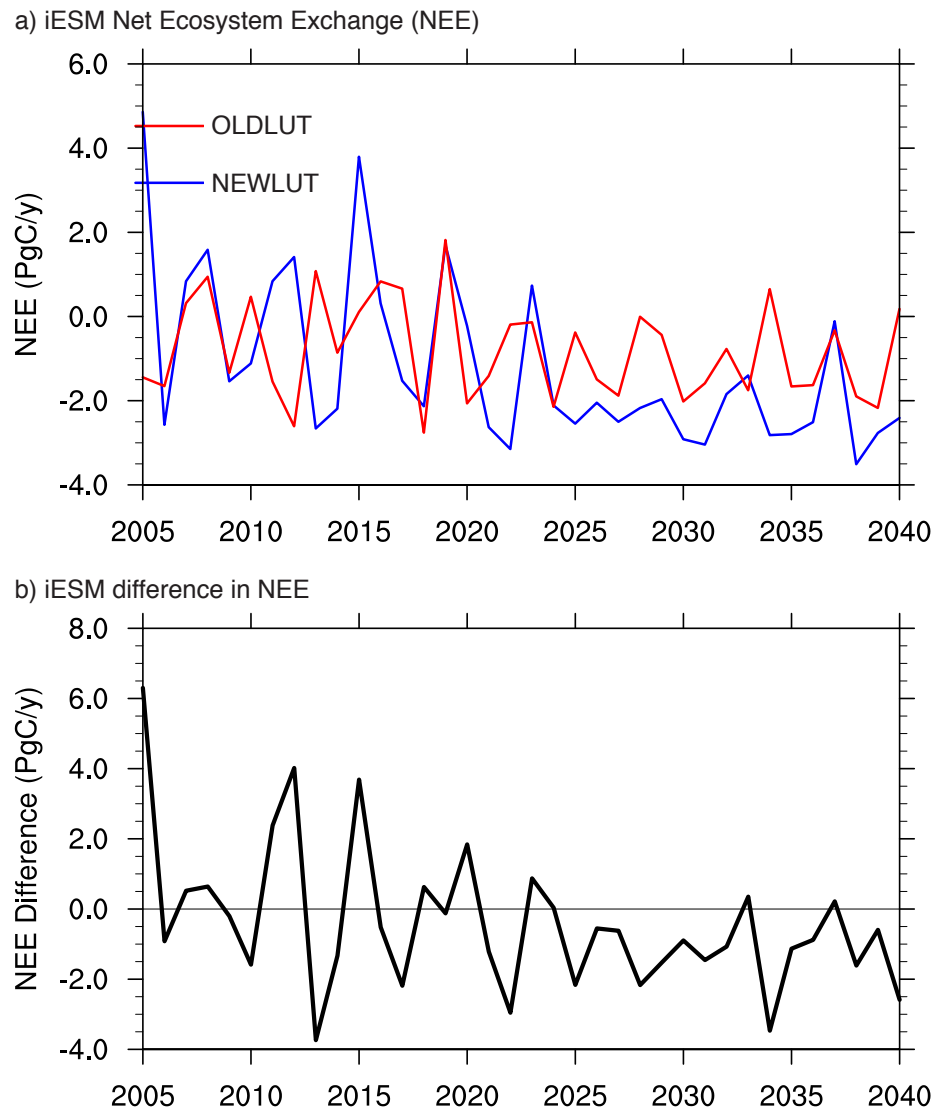


987 Figure 7. Integrated Earth System Model (iESM) land use and forest area. The GLM-NEWLUT
 988 forest and pasture data are nearly identical to the GLM-OLDLUT data and are not shown for
 989 clarity. Similarly, the GLM-NEWLUT cropland data track the GCAM-NEWLUT data, but with
 990 the same offset as for the GLM-OLDLUT data. CESM: Community Earth System Model.
 991 GCAM: Global Change Assessment Model. GLM: Global Land use Model.



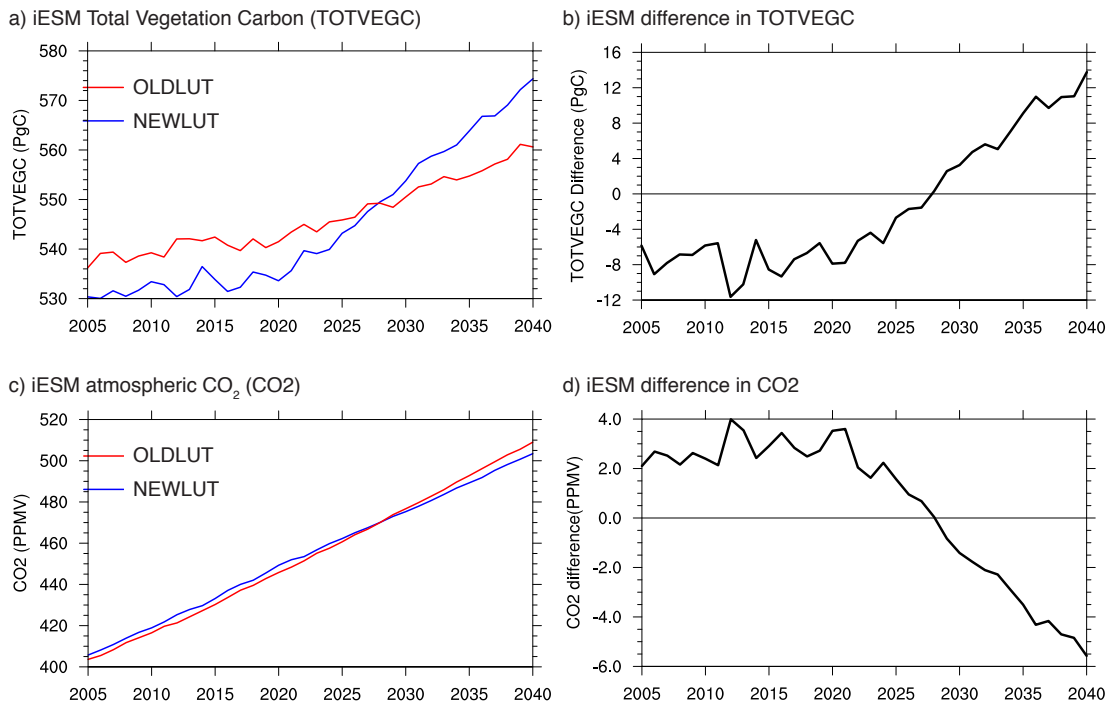
993
994

995 Figure 8. Spatial distributions of iESM increased forest Plant Functional Types (PFTs),
 996 decreased grass and shrub PFTs, and potential forest PFTs, as percentages of land area within
 997 each grid cell. a) Difference in 2040 forest PFT area (NEWLUT - OLDLUT). b) Difference in
 998 2040 grass plus shrub PFT area (NEWLUT - OLDLUT). c) Potential forest PFT area.
 999



1000
1001 Figure 9. Net Ecosystem Exchange (NEE) comparison between iESM simulations. a) NEE for
1002 each simulation. b) NEE difference (NEWLUT minus OLDLUT). These data show more land
1003 carbon uptake (negative NEE), associated with the additional trees, for the NEWLUT simulation
1004 during the afforestation period (2015 forward).

1005



1006

1007

1008 Figure 10. Comparison between iESM simulations of a-b) vegetation carbon and c-d)
1009 atmospheric CO₂ concentration. Differences are NEWLUT minus OLDLUT. Due to additional
1010 forest area, the NEWLUT simulation significantly increases vegetation carbon gain and
1011 decreases atmospheric CO₂ gain over the OLDLUT simulation.